New Specimens of the Multituberculate Mammal Sphenopsalis from China: Implications for Phylogeny and Biology of Taeniolabidoids

Authors: Mao, Fang-Yuan, Wang, Yuan-Qing, and Meng, Jin

Source: Acta Palaeontologica Polonica, 61(2) : 429-454

Published By: Institute of Paleobiology, Polish Academy of Sciences

URL: https://doi.org/10.4202/app.00117.2014

New specimens of the multituberculate mammal *Sphenopsalis* from China: Implications for phylogeny and biology of taeniolabidoids

FANG-YUAN MAO, YUAN-QING WANG, and JIN MENG

Mao, F.-Y., Wang, Y.-Q., and Meng, J. 2016. New specimens of the multituberculate mammal *Sphenopsalis* from China: Implications for phylogeny and biology of taeniolabidoids. *Acta Palaeontologica Polonica* 61 (2): 429–454.

Multituberculates are the most diverse and best known group of Mesozoic mammals; they also persisted into the Paleogene and became extinct in the Eocene, possibly outcompeted by rodents that have similar morphological and presumably ecological adaptations. Among the Paleogene multituberculates, those that have the largest body sizes belong to taeniolabidoids, which contain several derived species from North America and Asia and some species with uncertain taxonomic positions. Of the known taeniolabidoids, the poorest known taxon is *Sphenopsalis nobilis* from Mongolia and Inner Mongolia, China, represented previously by a few isolated teeth. Its relationship with other multituberculates thus has remained unclear. Here we report new specimens of *Sphenopsalis nobilis* collected from the upper Paleocene of the Erlian Basin, Inner Mongolia, China, during a multi-year field effort beginning in 2000. These new specimens document substantial parts of the dental, partial cranial and postcranial morphologies of *Sphenopsalis,* including the upper and lower incisors, partial premolars, complete upper and lower molars, a partial rostrum, fragments of the skull roof, middle ear cavity, a partial scapula, and partial limb bones. With the new specimens we are able to present a detailed description of *Sphenopsalis*, comparisons among relevant taeniolabidoids, and brief phylogenetic analyses based on a dataset consisting of 43 taxa and 102 characters. In light of the new evidence, we assess the phylogenetic position of *Sphenopsalis* and re-establish the family Lambdopsalidae. The monophyly of Taeniolabidoidea is supported in all our phylogenetic analyses. Within Taeniolabidoidea the Asian lambdopsalids and the North American taeniolabidids represent two significantly different trends of adaptations, one characterized by shearing (lambdopsalids) and the other by crushing and grinding (taeniolabidids) in mastication, which supports their wider systematic separation, as speculated when *Sphenopsalis* was named.

Key words: Mammalia, Multituberculata, Taeniolabidoidea, *Sphenopsalis*, Paleogene, Erlian Basin, Inner Mongolia, China.

Fang-Yuan Mao [maofangyuan@ivpp.ac.cn] and Yuan-Qing Wang [wangyuanqing@ivpp.ac.cn], Key Laboratory of Vertebrate Evolution and Human Origin, Institute of Vertebrate Paleontology and Paleoanthropology, Chinese Academy of Sciences, Beijing 100044, China.
Jin Meng [jmeng@amnh.org] (corresponding author), Division of Paleontology, American Museum of Natural History, Central Park West at 79th St., New York, NY 10024, USA.

Received 19 August 2014, accepted 29 January 2015, available online 16 February 2015.

Introduction

Four multituberculates have been reported from the Paleocene of the Mongolian Plateau: *Prionessus* Matthew and Granger, 1925, *Sphenopsalis* Matthew, Granger, and Simpson, 1928, *Lambdopsalis* Chow and Qi, 1978, and *Mesodmops* Missiaen and Smith, 2008. The first multituberculate specimen discovered in Paleogene deposits of Asia was an edentulous dentary collected from the Gashato Formation at Shabarakh Usu, Mongolia, by the Central Asiatic Expedition (CAE) in 1923, and was subsequently designated the holotype of *Prionessus lucifer* (Matthew and Granger, 1925). In 1925 additional specimens of *Prionessus lucifer* were discovered at the same locality, including upper and lower teeth, as well as fragmentary material on which *Sphenopsalis nobilis* was ultimately named (Matthew et al. 1928). About 50 years later, *Lambdopsalis bulla* from the Nomogen Formation in Inner Mongolia, which is the best known multituberculate species from the Mongolian Plateau, was named (Chow and Qi 1978). The craniodental material of *L. bulla* have been thoroughly studied by Miao (1986, 1988), and the ear region and postcranials by Miao among others (Miao and Lillegraven 1986; Miao 1988; Kielan-Jaworowska and Qi

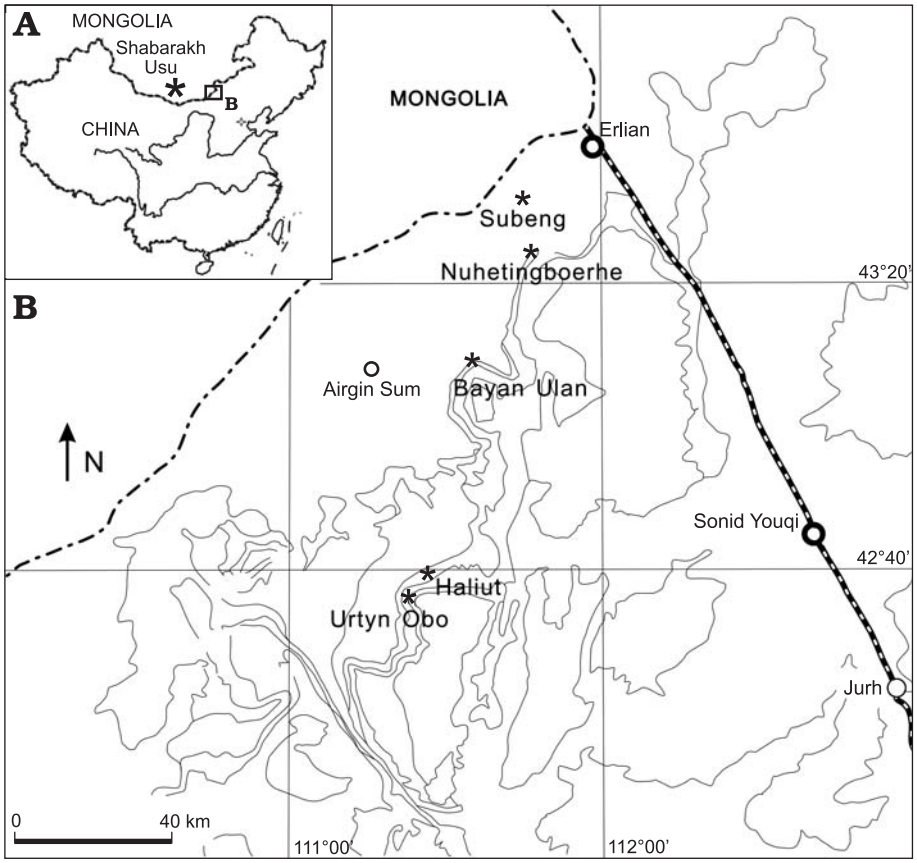

Fig. 1. Late Paleocene Gashatan localities for multituberculates in the Mongolian Plateau. **A**. Shabarakh Usu, Mongolia, where *Sphenopsalis nobilis* and *Prionessus lucifer* were first discovered. **B**. Erlian Basin, Inner Mongolia, China. *Lambdopsalis bulla, P. lucifer*, and *Mesodmops tenuis* were reported from Subeng (Missiaen and Smith 2008). *L. bulla* and *P. lucifer* were present in Nuhetingboerhe (Wang et al. 2010) and Bayan Ulan (Meng et al. 1998). *L. bulla*, *S. nobilis*, and *P. lucifer* were present in Haliut (Chow and Qi 1978) and Erden (Urtyn) Obo area (this study).

1990; Meng 1992; Meng and Wyss 1995). The fourth multituberculate known from the Mongolian Plateau is a ptilodontoid, *Mesodmops tenuis*, based on a few isolated teeth; the species has been reported from Subeng in the Erlian Basin (Missiaen and Smith 2008).

Prionessus and *Lambdopsalis* have been documented in the Nomogen Formation at several localities, including in the Nomogen district (Chow and Qi 1978), Bayan Ulan (Jiang 1983; Meng et al. 1998), Subeng (Jiang 1983; Meng et al. 2007; Missiaen and Smith 2008), and the Huheboerhe area (Wang et al. 2010). *Mesodmops* is so far known only from Subeng (Missiaen and Smith 2008) in the Mongolian Plateau (Fig. 1). Outside of the type locality at Shabarakh Usu, Mongolia (Matthew et al. 1928), a few teeth of *Sphenopsalis* were previously mentioned from the Haliut locality (Chow and Qi 1978) in the Nomogen district of Inner Mongolia, but descriptions of those specimens have yet to be published. Lastly, specimens referred to "*Sphenopsalis noumugenensis* sp. nov." were mentioned as coming from the Nomogen Formation of the Inner Mongolia (Jiang 1983), but this species has never been diagnosed or described.

The specialized tooth morphology of *Sphenopsalis* puzzled early workers regarding the taxonomic affinity of the genus (Matthew et al. 1928; Granger and Simpson 1929). These authors recognized the unique and peculiar tooth morphology of *Sphenopsalis*, which differs from that of *Taeniolabis,* and discussed the possibility that a wider systematic separation of the two genera may be necessary when the former became better known. The discovery of *Lambdopsalis* (Chow and Qi 1978) further complicated the issue, with Kielan-Jaworowska and Sloan (1979: 195) questioning its taxonomic validity and suggesting that *Lambdopsalis* was possibly a junior synonym of *Sphenopsalis*. Although studies by Miao (1986, 1988) provided sufficient evidence to affirm the taxonomic status of *Lambdopsalis bulla*, the systematic position of *Sphenopsalis* has not changed, in large part because of the limited number of specimens. Currently, *Sphenopsalis* is placed in the Taeniolabididae, a family that includes the North American *Taeniolabis* and *Catopsalis*, the Asian *Prionessus* and *Lambdopsalis*, and tentatively, the Late Cretaceous *Bubodens* (Kielan-Jaworowska et al. 2004).

Here we report on new specimens of *Sphenopsalis*, collected from the Nomogen Formation at a locality near the escarpment of Erden (Urtyn) Obo. The mammal assemblages from the Nomogen Formation in the Inner Mongolia, China, are collectively referred to as the Nomogen fauna, and represent the first late Paleocene fauna known from northern China (Chow et al. 1976; Chow and Qi 1978; Russell and Zhai 1987; Meng et al. 1998). Meng et al. (1998) considered the mammal assemblages from the Banyan Ulan, Gashato, Naran, and Nomogen localities to be age-equivalent, and as such collectively form the basis for the Gashatan Asian Land Mammal Age (ALMA) of East Asia. The Gashatan ALMA also includes Subeng, the stratigraphically lowest fauna in the Nuhetingboerhe area and the stratigraphically lowest fauna at the Erden (Urtyn) Obo area.

Table 1. Multituberculates from the late Paleocene localities of the Mongolian Plateau.

Locality	Horizon	Species included
Subeng, Erlian Basin, Inner Mongolia, China	Lower part of Nomogen Formation	*Prionessus lucifer*, *Lambdopsalis bulla*, *Mesodmops tenuis*
Nuhetingboerhe, Erlian Basin, Inner Mongolia, China	Lower part of Nomogen Formation	*Prionessus lucifer*, *Lambdopsalis bulla*
Haliut and Gonghudong in Erden (Urtyn) Obo area, Erlian Basin, Inner Mongolia, China	Lower part of Nomogen Formation	*Sphenopsalis nobilis*, *Lambdopsalis bulla*
Banyan Ulan, Erlian Basin, Inner Mongolia, China	Lower part of Nomogen Formation	*Lambdopsalis bulla*, *Prionessus lucifer*
Naran, Nemegt Basin, Mongolia	Naran and Zhigden members of the Naran Bulak Formation	*Prionessus lucifer*
Shabarakh Usu, Mongolia	Member I of the Gashato (Khashat) Formation	*Prionessus lucifer*, *Sphenopsalis nobilis*

In this study we first provide descriptions of new specimens of *Sphenopsalis nobilis*, then compare *Sphenopsalis* with other taeniolabidoid multituberculates, including the Asian *Lambdopsalis* and *Prionessus* and the North American *Taeniolabis* and *Catopsalis*, and follow up with phylogenetic analyses of multituberculates focusing on taeniolabidoids. Based on the new evidence, we further confirm that *Lambdopsalis* and *Sphenopsalis* are valid genera and that they are more closely related to each other than either is to any other multituberculate. Because of their unique and shared derived features, they stand distinct from other known multituberculates; thus, we revalidate the family Lambdopsalidae Chow and Qi, 1978 for these two morphologically advanced genera. The monophyletic Taeniolabidoidea now consist of at least two families: the Asian Lambdopsalidae and the North American Taeniolabididae. In addition, as the largest known multituberculate from Eurasia, the new specimens of *Sphenopsalis* and those of *Lambdopsalis* show a distinctive occlusal pattern that differs from that of the North American taeniolabidids and most other cimolodontans and lend additional support to the hypothesis that tooth morphology of multituberculate changed in association with generic richness and disparity in body size across the Cretaceous–Paleogene (K–Pg) transition, suggesting an adaptive shift towards increased herbivory that was little affected by the K–Pg mass extinction (Wilson 2013; Wilson et al. 2012).

Institutional abbreviations.—AMNH, American Museum of Natural History, New York, USA; IVPP, Institute of Vertebrate Paleontology and Paleoanthropology, Chinese Academy of Sciences, Beijing, China.

Geological setting and localities

Figure 1 shows the late Paleocene localities of the Mongolian Plateau where multituberculates have been reported, with localities in Inner Mongolia being illustrated with more details. Table 1 lists the known multituberculate species from each locality. Specimens of *Prionessus lucifer* and *Sphenopsalis nobilis* were first discovered from the Gashato Formation at Shabarakh Usu, Mongolia (Matthew and Granger 1925; Matthew et al. 1928). Dashzeveg (1988) also reported *Prionessus* from the Naran and Zhigden members of the Naran Bulak Formation at the Nemegt Basin, which was considered correlative to Member I of the Gashato Formation that generated the original Gashatan fauna.

The Nomogen fauna was originally known from the Nomogen Formation at the Haliut and Gonghudong localities, Inner Mongolia (Chow et al. 1976; Chow and Qi 1978). Fossils were collected from a celestite mine in a small area. Specimens of *Prionessus* and *Sphenopsalis* and the type specimens of *Lambdopsalis*, along with other typical Gashatan mammals, were collected from these localities. The Bayan Ulan fauna was from the basal beds in the Bayan Ulan section that is correlative to the upper part of the Nomogen Formation (Meng et al. 1998). Since the review of Russell and Zhai (1987), additional taxa, particularly small mammals, had been collected from the Bayan Ulan locality, and the assemblage was considered to be typical of the Gashatan fauna (Meng et al. 1994, 1998; Meng and McKenna 1998). The Bayan Ulan locality produced numerous specimens of *Lambdopsalis* and some of *Prionessus*, but *Sphenopsalis* has not been found in this site.

The Subeng locality was discovered in 1970s (Jiang 1983; Qi 1987; Russell and Zhai 1987; BGMRNMAR 1991; Meng et al. 1998), and a brief history about the investigation at this locality was summarized in Meng et al. (2007). *Prionessus* and *Lambdopsalis* were first reported from Subeng by Jiang (1983). Meng et al. (2007) listed two potentially new genera and species of ptilodontids from Subeng, and the ptilodontoid, *Mesodmops tenuis* was reported from this locality (Missiaen and Smith 2008). Despite of intensive collecting effort, *Sphenopsalis* is still unknown at Subeng.

In more recent years, extensive field investigations and collecting have been taking place in the Nuhetingboerhe area in the Erlian Basin (Meng et al. 2007; Wang et al. 2010, 2012; Fig. 1). In addition to other Gashatan mammals, *Prionessus* and *Lambdopsalis*, but not *Sphenopsalis,* were collected from this locality.

The Erden (Urtyn) Obo locality was known much earlier than other Paleogene localities in Inner Mongolia as it was first collected by the Central Asiatic Expeditions of the AMNH in 1928 (Granger 1928; Osborn 1929; Radinsky 1964; Qi 1990) and later by the joint expedition of China and Soviet Union (Chow and Rozhdestvensky 1960). However, most of the field

activities took place along the escarpment mainly formed by Eocene–Oligocene sediments. The upper Paleocene Nomogen beds lie in the lowland several kilometers on the north side of the escarpment. The first *Sphenopsalis* and *Lambdopsalis* specimens from the Nomogen beds were collected by Yaoming Hu and Jin Meng in 2000. In a follow-up study, Bowen et al. (2005) published a preliminary paleomagnetic sequence of the entire section of the Erden Obo, in which *Lambdopsalis* and *Sphenopsalis*, along with other typical Gashatan mammals were documented. In the following years, additional specimens of *Sphenopsalis* were collected from the Nomogen beds in the area, and all the specimens are described in this study. From the known data, it appears that *Sphenopsalis* and *Prionessus* had wider geographic distributions than *Lambdopsalis*, which has been reported only in localities in the Erlian Basin of Inner Mongolia.

Material and methods

Newly described specimens are housed in the collections of the IVPP, Chinese Academy of Sciences, Beijing and listed in "Referred new specimens" below. All specimens were prepared with the aid of dissecting needles to remove the surrounding matrix. We follow Kielan-Jaworowska and Qi (1990), Kielan-Jaworowska and Gambaryan (1994), and Kielan-Jaworowska et al. (2004) for postcranial terminology. Standard convention is followed in abbreviating tooth families as I, C, P, and M, with upper and lower case letters referring to upper and lower teeth, respectively. For general cusp formula and tooth structures, we follow Kielan-Jaworowska et al. (2004).

The optical photographs were taken using a Canon Mark III camera with a macro lens, and the SEM photographs were of uncoated specimens using a Hitachi S-3700N scanning electron microscope at the Key Laboratory of Vertebrate Evolution and Human Origin, IVPP. Dental measurements were taken using Mitutoyo digital calipers.

We performed cladistic analyses using PAUP4.0b (Swofford 2002), and employed the data matrix of Yuan et al. (2013), a recent multituberculate character-taxon matrix that used morphological characters from various sources, including Simmons (1993), Rougier et al. (1997), Weil (1998), Hahn and Hahn (1998a, b), Butler (2000), Kielan-Jaworowska and Hurum (2001), Kielan-Jaworowska et al. (2004), Butler and Hooker (2005), Luo et al. (2002, 2011) and Cifelli et al. (2013). We included the taeniolabidid *Catopsalis* in our analyses, which was not included in Yuan et al. (2013), and followed Rougier et al. (1997), Granger and Simpson (1929) as well as JM observations of specimens and casts housed in the AMNH for coding decisions. Codings for *Prionessus* are based on Matthew et al. (1928), Meng et al. (1998), and F-YM and JM personal observations on specimens housed in the AMNH and the IVPP. Specimens from the IVPP include those that were collected in the last decade. The total number of ingroup taxa is 41, of which 2 are haramiyidans and 39 are multituberculates. In contrast to the analysis of Yuan et al. (2013), we did not employ a hypothetical ancestor methodology in our analysis; we instead specify *Sinoconodon* and *Morganucodon* as outgroup taxa. We conducted analyses with all characters being treated as unordered as well as analyses in which some characters are ordered, following Yuan et al. (2013) (see also Phylogenetic analyses). The data matrix and character list are presented in SOM 1 and 2 in the Supplementary Online Material, available at http://app.pan.pl/SOM/app61-Mao_etal_SOM.pdf.

Systematic palaeontology

Order Multituberculata Cope, 1884

Suborder Cimolodonta McKenna, 1975

Superfamily Taeniolabidoidea Sloan and Van Valen, 1965

Families and genera included: Taeniolabididae Granger and Simpson, 1929 (*Taeniolabis* Cope, 1882, type genus; *Catopsalis* Cope, 1882). Lambdopsalidae Chow and Qi, 1978, which we re-established in this study (see below) (*Lambdopsalis* Chow and Qi, 1978, type genus; *Sphenopsalis* Matthew, Granger, and Simpson, 1928). We tentatively consider *Prionessus* as family incertae sedis for the reason given in the following discussion. Following Kielan-Jaworowska et al. (2004), we also tentatively refer the poorly known Late Cretaceous *Bubodens* Wilson, 1987 to Taeniolabidoidea. Its general morphology is more *Taeniolabis*-like in having inflated tooth cusps that bear horizontal wear facets on cusp tips.

Emended diagnosis.—The combination of the following features distinguishes Taeniolabidoidea from other multituberculates: including the largest known North American and Asian multituberculates (skull length in the Paleocene *Taeniolabis* reaching 16 cm); dental formula 2.0.1-2.2/1.0.1.2; tooth with gigantoprismatic enamel (shared with all Cimolodonta except Ptilodontoidea); snout short and wide with anterior part of zygomatic arches directed transversely, resulting in a square-shaped skull; frontals small, pointed posteriorly, almost or completely excluded from the orbital rim; the frontal deeply inserted between the nasals; I2 and I3 singlecusped; small or no diastema between I2 and I3; I3 on the margin of the premaxilla; having only one upper premolar (except for one taxon); P4 with one main cusp row and one root, long diastema between I3 and premolars; P4 and p4 strongly reduced in proportion to enlarged, multicusped molars and triangular in lateral view; p4 without oblique ridges and not laterally compressed to be bladelike; M1 having three rows of cusps with the lingual one extending for nearly the whole length of the tooth and bearing 7–9 cusps or more.

Remarks.—The emended diagnosis is modified from that of Kielan-Jaworowska et al. (2004). Taeniolabidoidea as a suborder was proposed and defined by Sloan and Van Valen (1965: 222) as: "including multituberculates in which the enamel of the lower incisor is restricted to the ventro-lateral surface of the tooth, producing a self-sharpening tooth similar to that of

rodents. The shearing premolars are reduced in proportion to the molars in all included genera except *Eucosmodon*". Since the proposal, whether taeniolabidoids form a natural group has been a matter of debate for decades (Clemens and Kielan-Jaworowska 1979; Kielan-Jaworowska 1974, 1980; Carlson and Krause 1985; Simmons 1993; Fox 1999, 2005; Kielan-Jaworowska and Hurum 2001; Kielan-Jaworowska et al. 2004). The complicated research history of the group may be reflected by the taxon name that is associated with multiple author names: "Superfamily Taeniolabidoidea (Sloan and Van Valen 1965), McKenna and Bell, 1997, Fox, 1999" (Kielan-Jaworowska and Hurum 2001: 417). Since the work of Fox (1999), the taxonomy that Taeniolabidoidea include only a monotypic family Taeniolabididae Granger and Simpson, 1929 has been widely accepted (Kielan-Jaworowska and Hurum 2001; Jaworowska et al. 2004; Fox 2005). The family includes mainly five genera: *Taeniolabis* Cope, 1882 (type genus), *Catopsalis* Cope, 1882, *Lambdopsalis* Chow and Qi, 1978, *Prionessus* Matthew and Granger, 1925, and *Sphenopsalis* Matthew, Granger, and Simpson, 1929. Kielan-Jaworowska et al. (2004) did not list all genera in the family for the reason that their work was intended to document only the Mesozoic taxa. These authors, however, tentatively assigned the poorly known Late Cretaceous *Bubodens* Wilson, 1987 to Taeniolabididae and provided by far the most up-to-date diagnosis for the superfamily and family. In our understanding the diagnosis, expanded from Kielan-Jaworowska and Hurum (2001), should be applicable to the Paleogene genera. Fox (2005) analyzed and discussed seven characters in detail that were used in various studies, primarily Simmons (1993), to diagnose Taeniolabidoidea that included Taeniolabididae and species belonging to Eucosmodontidae, Sloanbaataridae, and Djadochtatheriidae. Fox (2005) concluded that Taeniolabidoidea as previously defined (i.e., Simmons 1993) were not monophyletic and noted that Taeniolabidoidea functions as a taxon redundant with its single included family, Taeniolabididae in Kielan-Jaworowska and Hurum (2001). However, because their manuscripts were probably completed roughly around the same time so that Kielan-Jaworowska et al. (2004) and Fox (2005) were unaware of each other's work.

In light of the new specimens of *Sphenopsalis*, we are able to discuss some features that are relevant to the phylogenetic placement or taxonomy of *Sphenopsalis* and other taeniolabidoids. For instance, one of the diagnostic features used in the diagnosis for Taeniolabidoidea (Kielan-Jaworowska et al. 2004: 331) was: "Share strong, self-sharpening incisors that have enamel limited to the outer surface with most Djadochtatherioidea and Eucosmodontidae." As we will show below, this character does not seem to properly characterize *Sphenopsalis* and other Asian Paleocene taeniolabidoids. The focus of this study is to present the morphology of *Sphenopsalis*, assess its phylogenetic position, and re-establish the family Lambdopsalidae. A thorough review on the taxonomy and phylogenetic relationship of Taeniolabidoidea is beyond the scope of the present study. However, the new morphologic data and comparisons in the following sections allow us to clarify some features of taeniolabidoids that were unknown for taxa such as *Sphenopsalis* but were nonetheless used in the diagnosis of Taeniolabidoidea. With the re-establishment of Lambdopsalidae (see below) and the discussion on Taeniolabidoidea by Fox (2005), we hope that our emended diagnosis for Taeniolabidoidea can be justified.

Stratigraphic and geographic range.—Late Cretaceous and Paleocene of North America and Asia (Fox 1989, 1997; Kielan-Jaworowska and Hurum 2001).

Family Lambdopsalidae Chow and Qi, 1978

Type genus: *Lambdopsalis* Chow and Qi, 1978.

Included genera: *Sphenopsalis* Matthew, Granger, and Simpson, 1928.

Emended diagnosis.—Differ from other multituberculates, including the North American taeniolabidoids, in having a combination of the following features: tooth formula 2.0.1.2/1.0.1.2; upper incisors anteriorly positioned, simple and pointed, with circular cross-section, and lacking diastema between I2 and I3; long diastema between I3 and P4; M1 cusp formula 7:7:8, M2 cusp formula 1:2:4; occlusal surface of molars, particularly M2/m2 forming a sloped trench with a broad V-shape in distal view; M2 cusps crescentic, with the two medial cusps in the shape of an oblique, strong ridge and nearly twice the width of the lingual ones; lower incisor with circular cross-section; m1–2 cusp formula 5:4 and 3:2, respectively; m1 significantly narrower than m2, with distal end wedged in the notched mesial surface of m2; the two lingual cusps of m2 strongly crescentic and about twice the width of the buccal cusps.

Geographic and stratigraphic range.—Upper Paleocene (Gashatan) of Mongolia and China.

Genus *Sphenopsalis* Matthew, Granger, and Simpson, 1928

Type species: *Sphenopsalis nobilis* Matthew, Granger, and Simpson, 1928; see below.

Emended diagnosis.—As for the type and only known species.

Sphenopsalis nobilis Matthew, Granger, and Simpson, 1928

Figs. 2–13.

Type material: Holotype: AMNH 21736, a left M2 (Fig. 2A). Paratypes: Other specimens from the hypodigm, some reported and figured by Matthew et al. (1928), are considered paratypes following Article 72 in the International Code of Zoological Nomenclature (4th Edition); these include an anterior part of the left m2 (AMNH 21713; Fig. 2B) and an anterior part of m1 (AMNH 21715; Fig. 2C). We present photographs of those specimens (except for some very fragmentary bits) to make the type series of the species more clearly illustrated. We also include two specimens associated with the holotype and paratypes in the collection that were neither mentioned nor figured in Matthew et al. (1928) (Fig. 2D [AMNH 21719.001], E [AMNH 21719.002]).

Type locality: Shabarakh Usu, Mongolia.

Type horizon: Late Paleocene Gashato Formation.

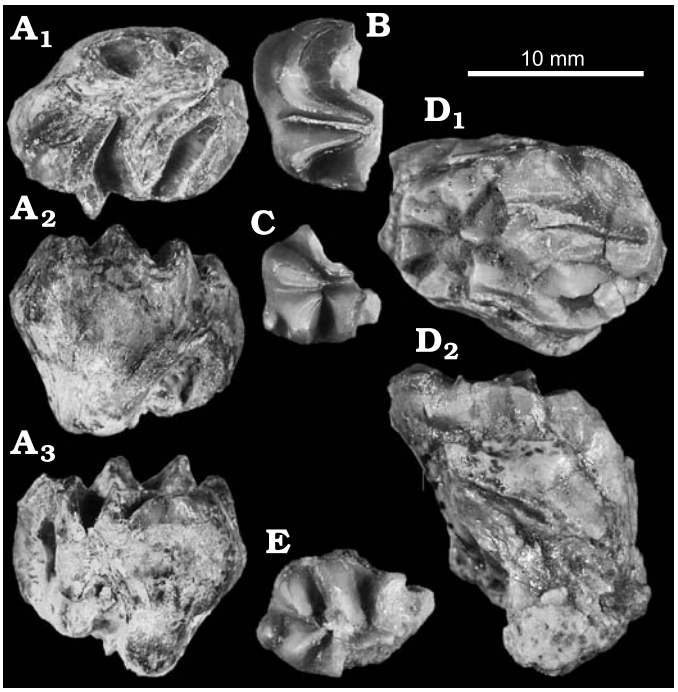

Fig. 2. Multituberculate mammal *Sphenopsalis nobilis* Matthew, Granger, and Simpson, 1928 from the late Paleocene Gashato Formation at Shabarakh Usu, Mongolia. **A**. Holotype (AMNH 21736), the upper left M2 in occlusal, lingual and buccal views (A_1–A_3). **B**. Paratype (AMNH 21713), anterior part of a left m2 in occlusal view. **C**. Paratype (AMNH 21715), anterior parts of a left m1 in occlusal view. **D**. AMNH 21719.001, broken ?M2 in occlusal (D_1) and lateral (D_2) views. **E**. AMNH 21719.002, anterior parts of a left m1 in occlusal view.

Material.—IVPP V19025, fragments of a skull including a left partial maxilla bearing complete M1–2, partial rostrum (the right side) with I2–3 and broken root of P4, partial right M1, anterior portions of both dentaries with basal parts of the incisors, skull fragment with the orbital crest, skull fragment with anterior portion of the left middle ear cavity, including a partial promontory of the petrosal and other bone fragments. All the specimens referred to IVPP V19025 were from a single individual; they were collected from a small (a square foot) pit where some elements were weathered out while others were preserved in situ in the sandstone. IVPP V19026, fragmentary right maxilla with M2 with damaged lingual cusp row; IVPP V19027, a tooth of uncertain identity (tentatively identified as a right m2 at an early stage of development); IVPP V19028, fragmentary right dentary with m2; IVPP V19029, several parts presumably from a single individual (with a similar preservation condition of IVPP V19025) including left maxilla with M1–2, partial right maxilla with broken M1–2, partial left dentary with damaged m2, fragmentary skull roof with frontals and other elements, and fragmentary bone that appears to be part of an inflated vestibule of the petrosal; IVPP V19030, fragments presumably from a single individual (with a similar preservation condition of IVPP V19025) including an anterior segment of the left dentary with broken incisor and the symphysis, the fragmentary left dentary with m2 and alveoli for m1, the left(?) mandibular condyle, proximal portion of the right scapulocoracoid, proximal portion of the left femur, the right femur with the proximal portion broken, nearly complete right tibia with the anterior side of the distal end broken, and various fragmentary vertebrae and bone chips; IVPP V19031, fragments presumably from a single individual, including distal left humerus, a segment of possible proximal portion of the left humerus with the head broken, left anterior part of the dentary with broken incisor (sectioned for enamel microstructure study), and partial right M2 (sectioned for enamel microstructure study); IVPP V19032, fragmentary left maxilla with M1–2 and left dentary with broken p4 and complete m1–2, from the same individual; IVPP V19033, left dentary with distal end of m1 and complete but deeply worn m2; IVPP V19034, anterior segment of the right dentary containing the incisor, with the tooth tip broken; IVPP V19035, partial left(?) lower incisor; IVPP V19036, fragments presumably from a single individual, including a partial right dentary with m2 and mandibular condyle with most of the neck; IVPP V19037, right dentary with the distal root of m1 and complete m2.

Emended diagnosis.—Differ from other multituberculates, including *Lambdopsalis,* in having the following combination of features: Largest known multituberculate in Eurasia (measurements in Table 2 and SOM 5); I2 and I3 subequal in size and shape and both incisors positioned at the anterior margin of the palate with I3 being slightly buccal; P4/p4 extremely small compared to the enlarged molars; a large incisive foramen on the palatal plane medial to the diastema between I3 and P4; M1 and M2 cusp formula 7:7:8 and 1:2:4; M1 lingual cusp row nearly as long as the medial one; humerus proportionally robust in relation to the femur. See Comparisons for more detailed differences between *Sphenopsalis* and *Lambdopsalis*.

Description.—*Upper incisor*: Of the two upper incisors of *Sphenopsalis*, I2 is slightly larger than I3 (Fig. 3; see Table 2 for tooth measurements). Both incisors are single rooted and single cusped, are only slightly compressed transversely, and the crown of either is covered with enamel for most of the labial surface. The alveolus for I3 is primarily housed in the premaxilla, but its posterior wall is formed by the maxilla (Fig. 3). The tip of I2 has a distinct wear facet, and

Table 2. Average tooth measurements (in mm) of *Sphenopsalis*. Abbreviations: L, mesiodistal length; N, number of specimens; W, buccolingual width; the asterisk indicates estimation from tooth alveolus. The actual measurements for each tooth are provided in the SOM 5.

Upper teeth (N)	I2 (1)		I3 (1)		P4 (1)		M1 (4)		M2 (4)	
Mean	L	W	L	W	L	W	L	W	L	W
	4.3	3.5	4.5	3.4	2.9	3.0*	16.4	8.3	13.3	12.2
Lower teeth (N)	i2 (3)		i3 (0)		p4 (1)		m1 (1)		m2 (8)	
Mean	L	W	L	W	L	W	L	W	L	W
	6.0	4.8			4.6	3.0	13.6	7.3	13.8	9.9

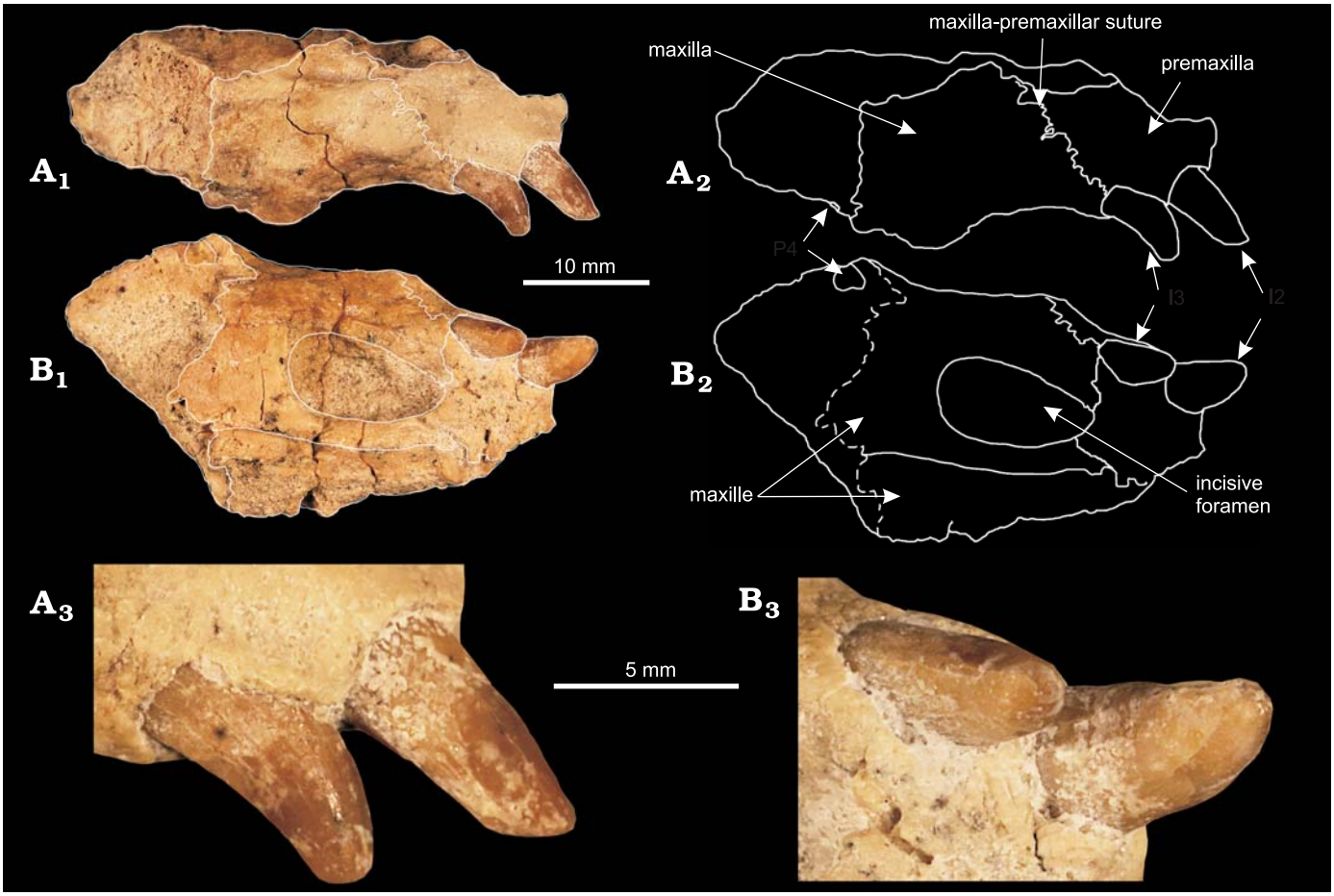

Fig. 3. Multituberculate mammal *Sphenopsalis nobilis* Matthew, Granger, and Simpson, 1928 (IVPP V19025) from the upper Paleocene Nomogen beds at the Erden (Urtyn) Obo locality, Inner Mongolia, China. Partial right rostrum with I2–3 in lateral (**A**) and ventral (**B**) views. A_2, B_2, explanatory drawings; A_3, B_3 details of A_1, B_1.

although I3 is more procumbent than I2, its lingual side also bears a wear facet at the tip, but smaller than that of I2. These wear facets do not indicate cutting motion of the incisors. The I3 of *Sphenopsalis* is positioned at the edge of the premaxilla, distal and slightly buccal to I2.

Upper premolar: A right portion of the rostrum is preserved (Fig. 3). On the ventral side of the rostrum a long diastema, about 20 mm in length, separates I3 and the alveolus for P4. The crown of the right P4 was broken but its root was preserved in the alveolus. From the circular cross-section of the root, it is clear that P4 is very small, simple and single-rooted. The maximum diameter of the root is about 3 mm.

Upper molars: Among the several upper molars referred here (Figs. 4, 5, 8), the best preserved and most informative are from IVPP V19025, an extensively preserved specimen that includes the nearly complete left M1–2 (Fig. 4), as well as the slightly damaged right M1 (Fig. 8E). All molars, including the lowers, have smooth enamel. The occlusal surface of the upper molars is concave ventrally when viewed buccally or lingually.

From slightly worn teeth (Figs. 4, 5, 8E, F) it is clear that the M1 crown is low and has a cusp formula 7:7:8. The buccal cusp row consists of seven cusps with the mesial two cusps being confluent but still recognizable. The mesial cusp continues mesiolingually as a ridge that connects to the mesial cusp on the medial row, and closes the furrow between the buccal and medial cusp rows. The distal cusp of the buccal row is the smallest, which is clear on the right M1 (Fig. 8E) but obscured by wear on the left M1 (Fig. 4). Cusps 3–5 on the buccal row are well delimited, and because their lingual sides are worn, the buccal sides of the cusps are higher. Cusps of the medial row are larger than those of the buccal and lingual rows and are generally wider than long. The penultimate cusp of the medial row is the largest, and the remaining cusps decrease in size mesially. Wear is deepest at the distal end of the crown, such that the distal cusps of the three rows form a large concave facet when deeply worn. The wear on M1 decreases mesially. The buccal side of each cusp in the medial row has a short ridge that extends mesially so that the buccal sides of adjacent cusps are connected after wear, whereas the lingual sides of the medial cusps are separated by a narrow and transverse groove (Fig. 4); this pattern remains even after the tooth was heavily worn. The wear facet on each cusp on the medial row can be divided into two parts: the buccal part continues on the buccal ridge, and is more extensive than the lingual part and faces ventro-

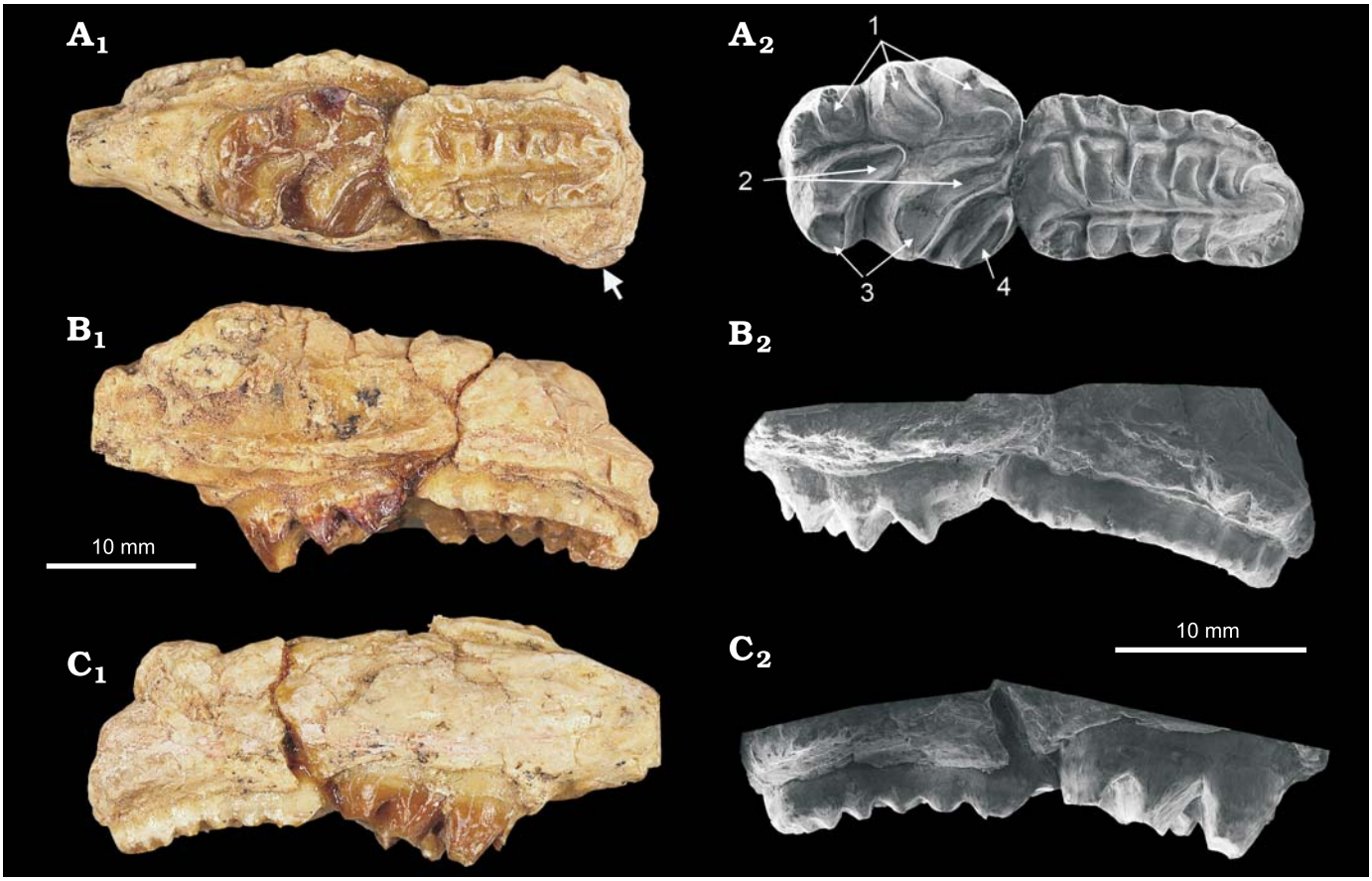

Fig. 4. Multituberculate mammal *Sphenopsalis nobilis* Matthew, Granger, and Simpson, 1928 (IVPP V19025) from the upper Paleocene Nomogen beds at the Erden (Urtyn) Obo locality, Inner Mongolia, China. Partial left maxilla with M1 and M2 in occlusal (**A**), medial (**B**), and lateral (**C**) views. The arrow indicates the broken anterior root of the zygomatic arch; wear facets: 1, on buccal sides of the lingual cusps of M2; 2, on lingual sides of the medial cusps of M2; 3, on buccal sides of the medial cusps of M2; 4, on the cusp of the buccal (external) row, which is aligned with the buccal wear facets of medial cusps of M2. Photographs (A_1–C_1), SEM images (A_2–C_2).

buccally. The lingual part is primarily at the tip of the cusp but slightly inclines to face ventrolingually. The lingual cusp row is slightly shorter than the medial row; its cusps decrease in size mesially and are transversely narrow but mediodistally long. After wear the lingual cusps become almost confluent to form a narrow crest (Fig. 5). The wear facets of the lingual cusps are inclined, facing ventrobuccally.

The M2 cusp formula is 1:2:4. The crown differs from that of M1 in being wider but shorter and higher, and in having reddish pigmentation on the enamel surface, similar to that of *Lambdopsalis* (Miao 1988). The pigmentation is concentrated in a thin layer of the outermost parts of the enamel of the tooth, but its composition and mechanism of formation are unknown. In contrast to M1, the M2 cusps are more crescentic, and the medial and lingual rows form a broad trench that is broadly V-shaped in distal view.

The single cusp of the buccal row is distinctive and situated at the mesiobuccal corner of the tooth (Figs. 4, 5, 8), and in all specimens at hand is smaller than its homologue in the holotype (Fig. 2A). The buccal cusp is crest-like and oriented mesiolingually-distobuccally, oblique to the long axis of the tooth. It has a convex mesiobuccal surface and a flat distolingual surface, and is separated from the mesial cusp of the medial row by a deep groove. Unlike the M1, where two furrows were comfined by three cusp rows, the M2 has only one central furrow, which is aligned distally with the furrow between the medial and lingual cusp rows of M1. The medial cusp row forms most of the buccal side of the M2. The mesial cusp on the medial row is situated slightly distolingual to the buccal cusp and extends mesiolingually as a strong, crescentic ridge that connects with the ridge from the mesial cusp on the lingual cusp row. The connection of the ridges mesially closes the furrow between the medial and lingual cusp rows. In the specimens at hand this cusp is relatively smaller than that of the holotype. The distal cusp of the medial row is higher than the mesial one, and it similarly extends distolingually as a strong ridge that is parallel to that of the mesial cusp. The two cusps are completely separated by a deep and narrow valley. The mesial cusp and ridge are worn more deeply than the distal one. In both cusps, the wear facet is divided into the buccal and lingual parts. The buccal part is primarily on the cusp tip and faces slightly ventrobuccally, and the lingual facet is primarily on the elongate ridge that is much larger and oblique, facing ventrolingually (Fig. 4). In more deeply worn M2s, such as the holotype, these two wear facets are confluent. The wear facet on the single cusp of the

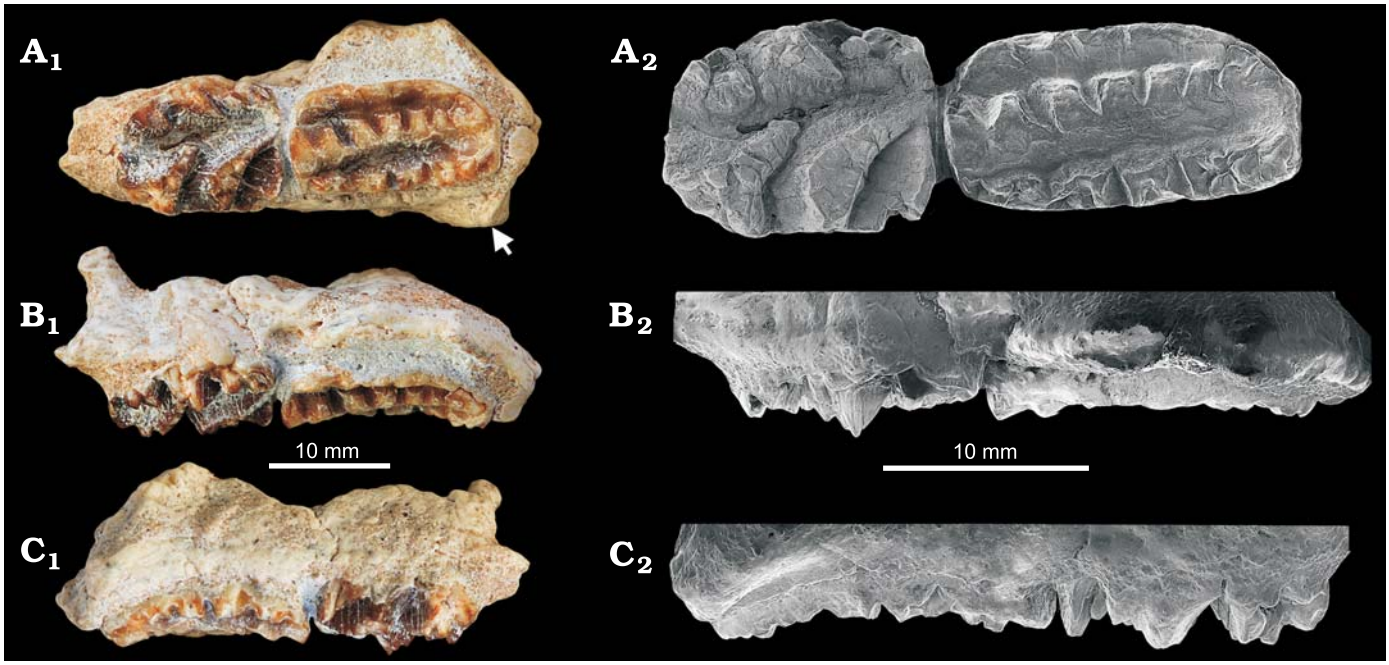

Fig. 5. Multituberculate mammal *Sphenopsalis nobilis* Matthew, Granger, and Simpson, 1928 (IVPP V19032) from the upper Paleocene Nomogen beds at the Erden (Urtyn) Obo locality, Inner Mongolia, China. Left upper molars (M1–2) from the same individual as the lower ones in Fig. 7 in occlusal (**A**), medial (**B**), and lateral (**C**) views. The arrow indicates the broken anterior root of the zygomatic arch. Photographs (A_1–C_1), SEM images (A_2–C_2).

external (buccal) row is aligned with the buccal wear facets of the medial cusps; thus, although the single buccal cusp is considered as from a different cusp row, it functions as if it was a mesial cusp of the medial cusp row.

The lingual cusp row of M2 consists of 4 cusps that are smaller and lower than the two medial cusps (Figs. 4, 5, 8). The base of each lingual cusp, except for the distal one, extends mesially, but they do not form strong ridges in the case of the medial cusps. In the holotype, the mesial cusp is small and subconical, whereas in IVPP V19025, the cusp is larger and continues mesiobuccally as a curved ridge to join the ridge of the mesial cusp of the medial row. The second cusp is the largest and tallest of the four lingual cusps. The distal cusp in the holotype is large and long, but in IVPP V19025 the homologue cusp is the smallest and in a form of transverse crest at the distolingual end of the tooth. Wear facets develop exclusively on the buccal side of each lingual cusp, but particularly on the mesial three cusps. These wear facets are oblique to the long axis of the crown, parallel to one another, but are not connected. The central furrow is wider mesially than distally and is open distally.

Lower incisor: The lower incisor is elongate with enamel restricted to the buccal side of the crown (Fig. 6). The tip of the incisor was broken on all specimens in collection. From the cross section revealed by broken incisors (IVPP V19025) and the relatively complete incisor with its medial side exposed (IVPP V19034), the incisor is determined to be nearly circular in cross section, being only slightly compressed transversely. The thickest portion of the lower incisor is within the region of the symphysis, and the tooth gradually tapers mesially and distally. The distal end of the tooth is open, revealing a hollow pulp cavity. The enamel does not extend the entire length of the incisor, but rather is restricted to the buccal side of the anterior portion of the tooth, with part of the enamel extends on the incisor body that is in the jawbone. There is no distinct boundary between the crown and the root, but the distal portion bearing no enamel may be considered as the root. The posterior extent of the incisor within the dentary cannot be accurately determined, but it likely extended to the level of p4. The enamel bears a reddish pigmentation, similar to that seen on the permanent incisor of *Lambdopsalis* (Miao 1986). The incisor has the gigantoprismatic enamel, which will be presented in a separate study.

Lower premolar: An incomplete p4 is preserved in IVPP V19032 (Fig. 7). The mesial part of the tooth is broken, but the remainder indicates that p4 is a small, single-rooted tooth with a simple crown that is transversely compressed and aligned with the lingual cusp row of m1.

Lower molars: In the original report by Matthew et al. (1928), a fragmentary left m1 (AMNH 21715) was reported (Fig. 2C), and a second incomplete left m1 (AMNH 21719.002; Fig. 2E) was also included in the hypodigm but was not figured. Because only the anterior half of m1 is preserved in both specimens, the cusp formula has until now remained unknown. The m1 (IVPP V19032) in the current collection is complete and has a cusp formula 5:4 (Fig. 7). The buccal cusps are smaller and lower than the lingual ones, but the size difference is not so dramatic when compared to those on the buccal and lingual cusp rows of m2. The mesial cusp of the buccal row is small; it is clearly present in AMNH 21715 and 21719.002 (Fig. 2), which are lightly worn, but is

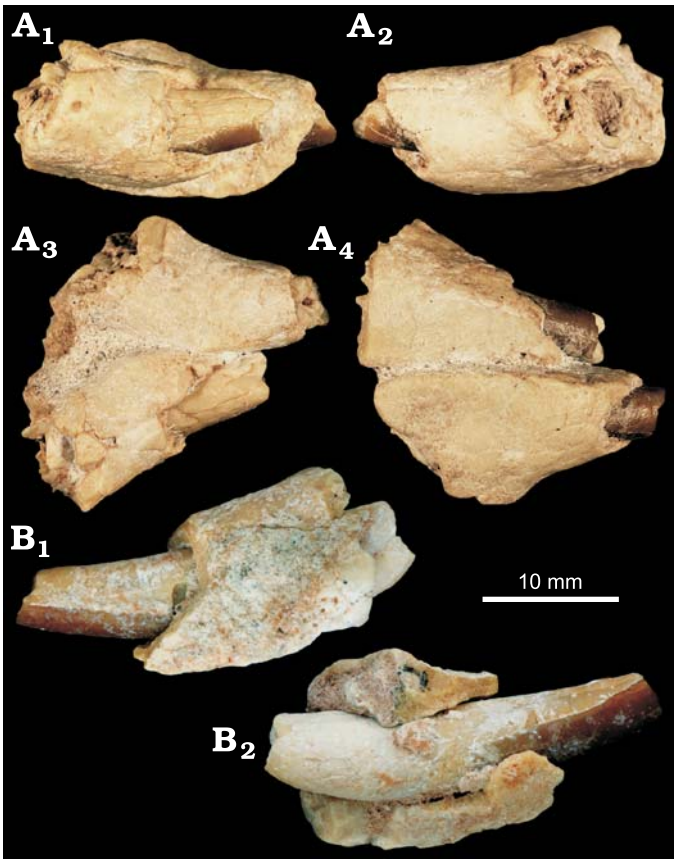

Fig. 6. Lower incisors of multituberculate mammal *Sphenopsalis nobilis* Matthew, Granger, and Simpson, 1928 from the upper Paleocene Nomogen beds at the Erden (Urtyn) Obo locality, Inner Mongolia, China. **A**. IVPP V19025, symphysis of mandibles with partial incisors in lateral right (A_1) and left (A_2), dorsal (A_3), and ventral (A_4) views. **B**. IVPP V19034, right incisor in medial (B_1) and lateral (B_2) views.

obscured by wear and poor preservation in IVPP V19032 (Fig. 7). Cusps 2–4 of the buccal row are subequal and each has a short ridge at the distolingual side that extends distolingually along the central valley. The cusps of the lingual row increase in size and height distally to the fourth cusp, which is of similar height to the mesial cusp on the lingual row of m2. The blunt ridges from the lingual cusps extend distobuccally along the central furrow. At the distal end of the tooth there is a distally convex ridge connecting the distal lingual and buccal cusps. Compared to m2, m1 is much narrower, as in *Lambdopsalis* (Miao 1986), and it is also slightly shorter than m2, differing from those in other taeniolabidoids.

The current collection contains several m2s that are well preserved (Figs. 7, 8). The m2 has a cusp formula 3:2 (Fig. 7) and in occlusal view narrows distally. Similar to M2, m2 also has the reddish pigmentation. The occlusal surface of m2 is not flat, but rather forms a broad trench that in distal view is V-shaped. In relatively unworn m2s (e.g., IVPP V19030; Fig. 8B), the cusps of both rows decrease in size and height distally and the central furrow is deep and narrow; with wear, the cusps become subequal in height and the occlusal surface becomes relatively flat (IVPP V19033; Fig. 8G). As seen in IVPP V19033, in which the lingual part of the dentary has been broken away, m2 has two robust roots that are positioned mesiodistally and gradually taper ventrally (not figured). The buccal cusp row of m2 has three cusps, of which the mesial one has a ridge that extends distally along the central furrow. The second cusp is the largest in the row and bears a mesial ridge that extends to the distobuccal base of the mesial cusp, and the two cusps are separated by a deep, diagonal groove. Distally, the second cusp is connected to the ultimate cusp by both lingual and buccal ridges, such that a concavity is formed between the two cusps (see seen in Fig. 8A, D_1, I). The lingual side of each buccal cusp has an oblique wear facet that faces dorsolingually. The longitudinal groove is narrow and is closed distally by a low ridge that connects the distal cusps of the lingual and buccal rows, as in *Lambdopsalis* (Miao 1988; F-YM personal observations).

The lingual row of m2 consists of two large cusps that account for about two thirds of the tooth width (Figs. 7, 8). The two cusps are strongly crescentic with buccal crests extending distally along the central furrow. The mesial lingual cusp is higher and larger than the distal cusp, but the distobuccal crest of the latter is longer and extends distally and buccally; it eventually joins the base of the distal buccal cusp and closing the distal end of the narrow central furrow. A pocket is formed at the distolingual side of the distal cusp.

Among the specimens of *Sphenopsalis* from Erden (Urtyn) Obo, there is a peculiar tooth (IVPP V19027; Fig. 8F) of uncertain identity. The tooth is of light color and bears thin enamel. Because this tooth was entirely within bone and excavated by preparation, it is likely a tooth at a very early stage of development, and the morphology and arrangement of cusps and crests suggest that it is most likely a right m2, but unlike m2 of *Sphenopsalis*, the tooth is much shorter and lacks the reddish pigmentation. The lingual cusp row, as interpreted here, is much longer than the buccal one, The cusps and crests are sharp and are unworn. Similar to m2, the lingual cusps are at least twice the width of the buccal ones. The mesial cusp is a sharp crest that extends more mesially than the buccal cusps, which is similar to that of m2 (IVPP V19037; Fig. 8A) but at a greater degree. Unlike m2, there is a sharp, isolated cusp at the distolingual end of the tooth. The width of the tooth is close to that of an adult m2 but its length is only a half of an adult m2.

Dentary and skull fragments: Several fragmentary dentaries and skull bones included in the current collection provide limited but informative anatomical information on the cranium of *Sphenopsalis*. The symphysis, preserved on the fragmentary left dentary (IVPP V19030) and several additional specimens (Fig. 6), is unfused, implying mobility between the two dentaries in life. The anterior end of the coronoid process is positioned at the buccal side of m2 as shown by its broken base in IVPP V19032 (Fig. 7). Additional, incomplete dentaries (not figured) demonstrate that, the dentary has a long condylar process that continues posteriorly to the mandibular condyle (preserved in two fragmentary dentaries, IVPP V19036). The condyle has a smooth surface with its dorsal portion being bulbous. In posterior view, the

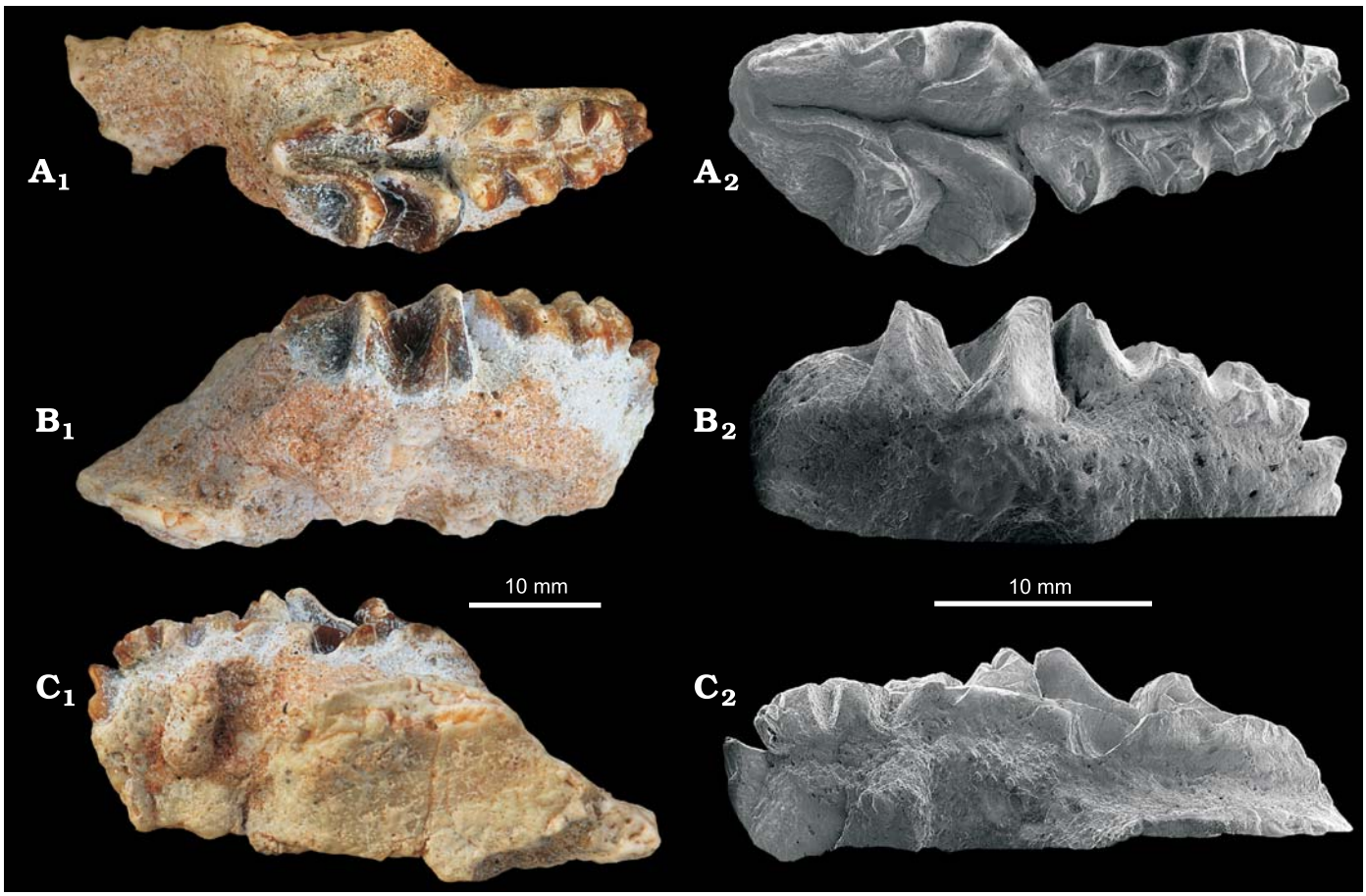

Fig. 7. Multituberculate mammal *Sphenopsalis nobilis* Matthew, Granger, and Simpson, 1928 (IVPP V19032) from the upper Paleocene Nomogen beds at the Erden (Urtyn) Obo locality, Inner Mongolia, China. Left lower cheek teeth (p4–m2) from the same individual as in Fig. 5 in occlusal (**A**), medial (**B**), and lateral (**C**) views. Photographs (A_1–C_1), SEM images (A_2–C_2).

condyle is not symmetrical, with the lateral side being dorsoventrally thicker. The medial surface of the condylar process is smooth, whereas the buccal surface bears a ridge that runs nearly parallel to the ventral border of the mandible.

The partial rostrum (most of the right half) (IVPP V19025; Fig. 3) is short, broad and low, as in *Lambdopsalis* and other taeniolabidoid multituberculates where the skulls were known (Kielan-Jaworowska and Hurum 2001; Kielan-Jaworowska et al. 2004). The width of the right part of the rostrum, measured between the curving point of the rostrum anterior to the P4 alveolus and the medial border of the maxilla on the palate, is about 16 mm. The premaxilla and maxilla are thick and nearly fused, although a vague suture is still discernible laterally. The premaxilla supports an anterior process, most of which is broken away, except for a small lateral part which projects anterodorsally. On the dorsal side of the rostrum and posterior to the premaxilla process, there is a concave area marking the point of articulation with the nasal; the bone is broken posterior to the concave area, revealing the termination of the I2 root. The premaxilla-maxilla suture intersects at the posterior side of I3 alveolus.

On the lateral side of the rostrum, the maxilla forms a knob-like protuberance posterodorsal to the I3 alveolus. The infraorbital canal is not preserved, but a groove anterior to its presumed position runs anteriorly on the lateral surface of the maxilla toward the protuberance. The groove was likely left by the infraorbital blood vessels and nerve. The anterior root of the zygoma appears to have originated at the anterior half of M1; this condition is also supported by the left maxilla bearing M1–2 (Figs. 4, 5). A short suture is developed on the dorsolateral edge of IVPP V19025, and probably represents the maxilla-nasal suture, or possibly the maxilla-frontal suture; if it is the former, then the nasal would have been extensive, extending posteriorly to the level of the anterior root of the zygoma.

In ventral (palatal) view, the premaxilla is rugose medial to the incisors. The most distinctive feature of the palate of *Sphenopsalis* is the large incisive foramen (Fig. 3), contrasting with the relatively small incisive foramen in *Lambdopsalis* (Miao 1988) and *Prionessus* (Meng et al. 1998). The foramen is immediately posteromedial to I3 and is primarily located within the maxilla, with only a minor contribution of the premaxilla at its anterior wall. The incisive foramen of *Sphenopsalis* measures 13.4 mm long and 7.4 mm wide at its maximum. The lateral wall of the incisive foramen, formed by the maxilla, is a steep but smooth surface that extends dorsally and faces ventromedially. The medial side of the incisive foramen is a

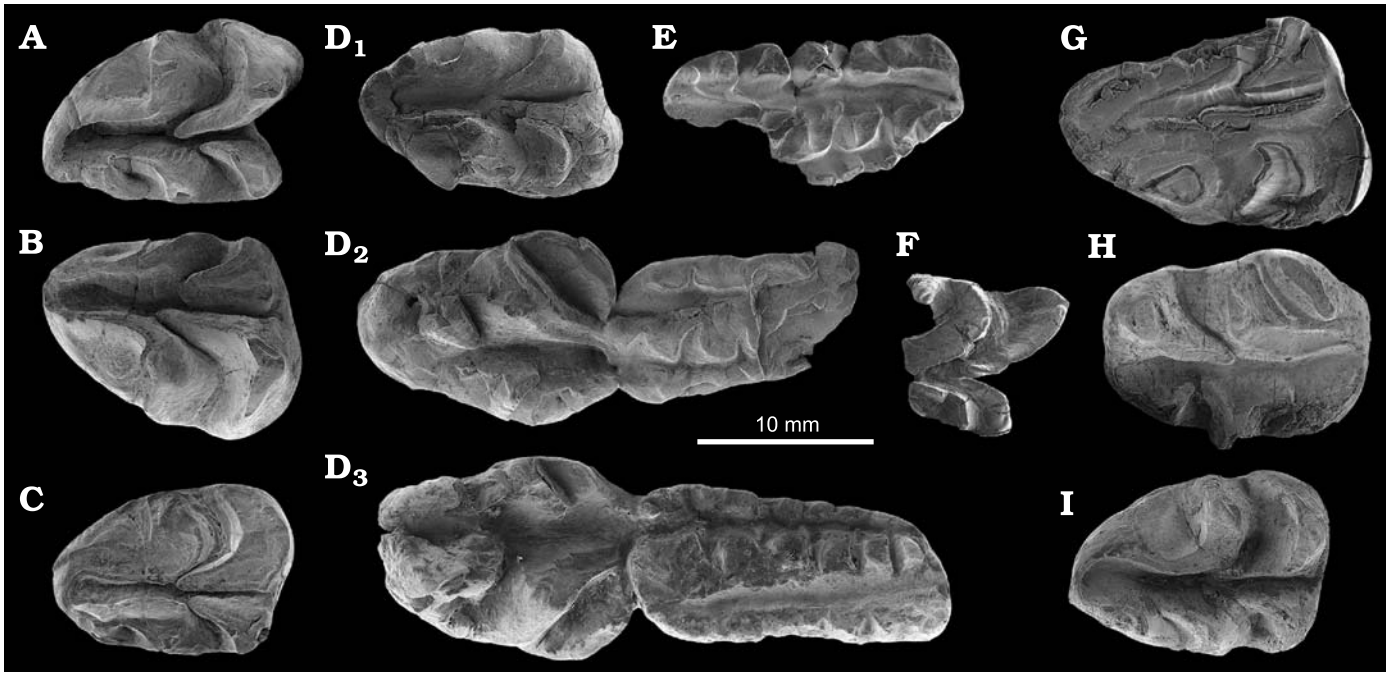

Fig. 8. Occlusal views of molars of multituberculate mammal *Sphenopsalis nobilis* Matthew, Granger, and Simpson, 1928 from the upper Paleocene Nomogen beds at the Erden (Urtyn) Obo locality, Inner Mongolia, China. **A**. IVPP V19037, right m2. **B**. IVPP V19030, left m2. **C**. IVPP V19028, right m2. **D**. IVPP V19029, right m2 (D_1), right M1–2 (D_2), left M1–2 (D_3). **E**. IVPP V19025, right M1, which belongs to the same individual as in Fig. 4. **F**. IVPP V19027, a developing right m2? **G**. IVPP V19033, a deeply worn left m2. **H**. IVPP V19026, right M2. **I**. IVPP V19036, right m2.

narrow bar, which is thick and has a rounded surface. The enlarged incisive foramen is not equivalent to any of the palatal vacuities that occur in some multituberculates, such as *Sloanbaatar* (Kielan-Jaworowska 1969), *Bulganbaatar* and *Nemegtbaatar* (Kielan-Jaworowska 1974), *Stygimys* (Sloan and Van Valen 1965) and *Ptilodus* (Simpson 1937). These palatal vacuities usually occur more posteriorly and medial to the premolars and molars, and where the suture is known the palatal vacuities are commonly between the maxilla and the palatine. The palatal vacuities do not occur in *Prionessus* (Matthew et al. 1928) and *Lambdopsalis* (Miao 1988). The posterior part of the palate was broken. The P4 alveolus was partly preserved in the broken maxilla at the lateral-most edge of the preserved specimen (Fig. 3).

The current collection includes a fragmentary skull roof with an incomplete orbital region (IVPP V19025; Fig. 9A). In dorsal view, the orbital region is characterized by having a narrow strip that is delimited medially by a suture on the roof of the skull fragment. This bony stripe is broken anteriorly so that it is not certain about its nature. By position, it could be part of the nasal or the maxilla, but more likely the latter. This bony stripe cannot be part of the frontal. Posterior to the broken "postorbital process" is a rounded notch that leaves a shallow grooved surface on the bony roof; we tentatively identify the notch as part of the postorbital foramen. The posterior part of this skull fragment should be the parietal, which is a thick bone.

A second specimen, IVPP V19029, from a different individual, includes part of the skull roof with what are interpreted here as the posterior parts of the frontals and anterior parts of the parietals (Fig. 9B). The frontals converge posteriorly as in other taeniolabidoids, and the anterolateral parts of the parietals curve ventrally, forming a blunt ridge that defines the anterodorsal border of the temporal region of the skull. If our interpretation is correct, then the narrowest part of the skull roof occurs at the anterior temporal region.

A third skull fragment, IVPP V19025, preserves the left portion of the pterygoid region and anterior part of the middle ear cavity (Fig. 10). The pterygoid forms the posterior portion of the lateral wall of the choanae. The preserved portion of the promontorium is straight and bulged, with its anterior pole extending anteromedially. The ventral surface is smooth, with steep medial and gently sloped lateral sides. The promontorium was broken at its posterior part, revealing the thick-boned cochlear house that in life enclosed the cochlea of the inner ear. The endocast shows a straight cochlear canal with a rounded cross-section. On the medial side of the broken posterior part of the promontorium is an incomplete foramen for the facial nerve. Owing to the breakage, the foramen can be traced to the dorsal side of the petrosal on the floor of the braincase. On the anterolateral side of the promontorium is a large rounded bony surface: based on its anatomical position, we interpret this recess as the fossa for the tensor tympani muscle (Wible and Rougier, 2000). This recess is much more expanded than that in other multituberculates where the middle ear cavity is known (e.g., *Kryptobaatar*; see Wible and Rougier 2000) and is significantly different from the middle ear of *Lambdopsalis*. Notwithstanding the several cracks in the bone, there is no fenestration in the tensor tympani fossa, and the middle ear

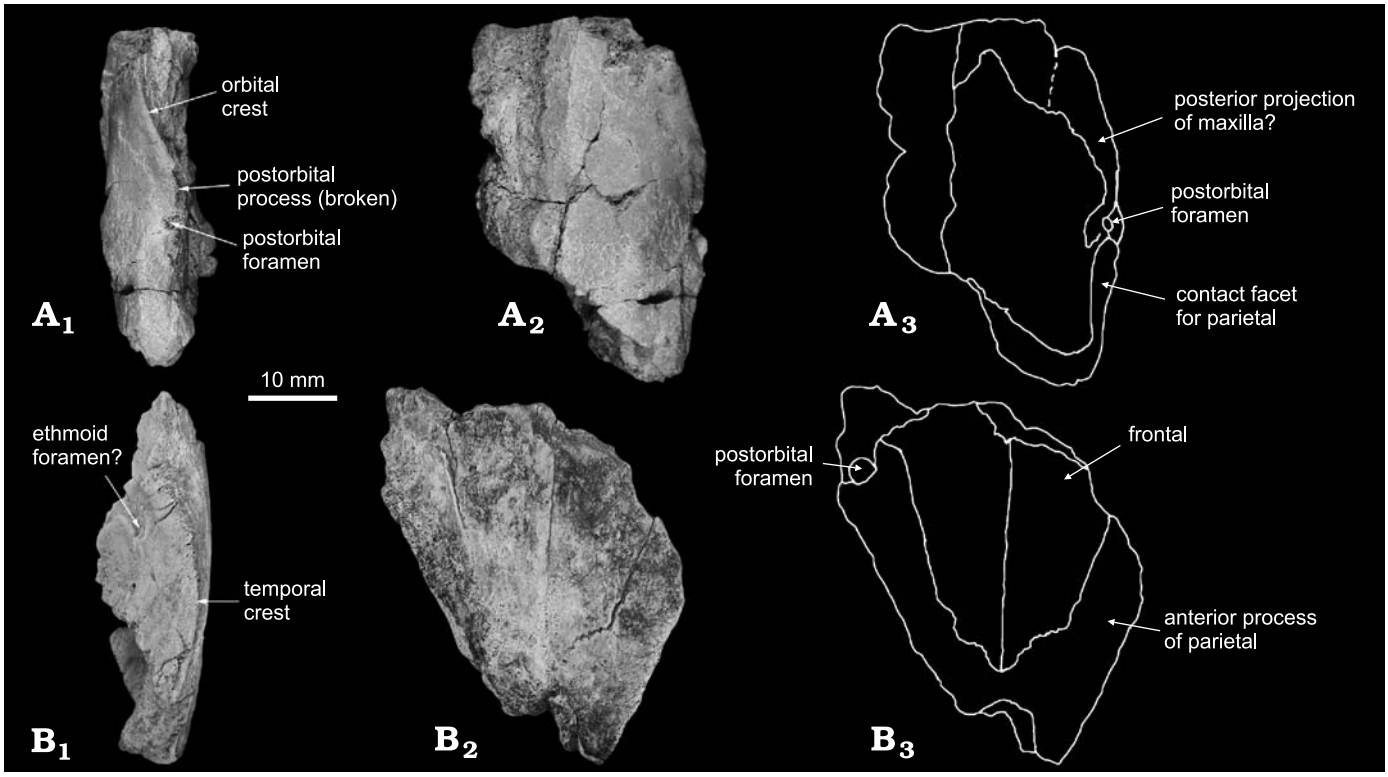

Fig. 9. Skull fragments of multituberculate mammal *Sphenopsalis nobilis* Matthew, Granger, and Simpson, 1928 from the upper Paleocene Nomogen beds at the Erden (Urtyn) Obo locality, Inner Mongolia, China. **A**. IVPP V19025, skull fragment showing the orbital crest in lateral (A_1) and dorsal (A_2, A_3) views. **B**. IVPP V19029, skull fragment showing the temporal crest in lateral (B_1) and dorsal (B_2, B_3) views. The anterior end of each element is toward upside. Photographs (A_1, A_2, B_1, B_2), explanatory drawings (A_3, B_3).

cavity in this region is completely roofed by bone. The anterior edge of this concave area is extended more anteriorly than the anterior tip of the promontorium. The composition of the bony roof for the tensor tympani fossa is unclear, but it must be primarily from the petrosal, judging from its relationship with the promontorium.

A final fragment, IVPP V19029, preserves an inflated vestibule, similar to that of *Lambdopsalis* (Fig. 10B). This bony element has a rough external surface and a roughly spherical inner surface. The best interpretation of this element is that it represents the bony shell of the inflated vestibule of the petrosal. By its absolute size, it is larger than the vestibule of *Lambdopsalis* (Miao 1988; Meng and Wyss 1995), but relative to the skull size as inferred from the teeth and preserved cranial parts of *Sphenopsalis,* it is propotionally less inflated than that of *Lambdopsalis*. Although an inflated vestibule is a common figure in multituberculates (Miao 1988; Meng and Wyss 1995; Fox and Meng 1997), the hypertrophic condition in *Lambdopsalis* and in *Sphenopsalis*, if our identification of the structure here is correct, would be unique among multituberculates.

Scapulocoracoid: The proximal right scapulocoracoid (IVPP V19030, Fig. 11A) shows a distinct scapular spine and infraspinous fossa, but it is difficult to determine whether the supraspinous fossa is present. The acromion is broken, but the base of the coracoid is present, and is not completely fused to the scapula, with the suture between the two elements remaining discernible. The distal tip of the coracoid is broken so that its original size is unknown, but the basal portion of the coracoid is broad and contributes to the anterior part of the glenoid fossa. The glenoid fossa is shallowly concave and has an oval outline with the long axis parallel to the scapular blade; it measures 16.8 mm long and 11.3 mm wide. With the scapula orientated in anatomical position, the glenoid fossa would face primarily ventrally. In general, the preserved portion of the scapulocoracoid is similar to that of *Lambdopsalis* (JM personal observations) and other multituberculates where the structure is known (Simpson 1928; McKenna 1961; Clemens and Kielan-Jaworowska 1979; Jenkins and Weijs 1979; Krause and Jenkins 1983; Kielan-Jaworowska 1989; Kielan-Jaworowska and Gambaryan 1994; Sereno and McKenna 1995).

Humerus: The present collection includes an incomplete left humerus preserving parts of both the proximal and distal ends (IVPP V19031; Fig. 11B). Although the two segments probably belong to the same individual (they were collected from the same pit), a reconstruction of the entire humerus is not possible, as the diaphysis is largely missing, and an estimate of the degree of humeral torsion accordingly cannot be made. The images in Fig. 11 display the general, not the precise, relationship of the humerus fragments. It is certain, however, that the humerus is robust, with the proximal and distal ends being transversely broad, suggesting fossorial adaptations. The posterior crest is well developed and the

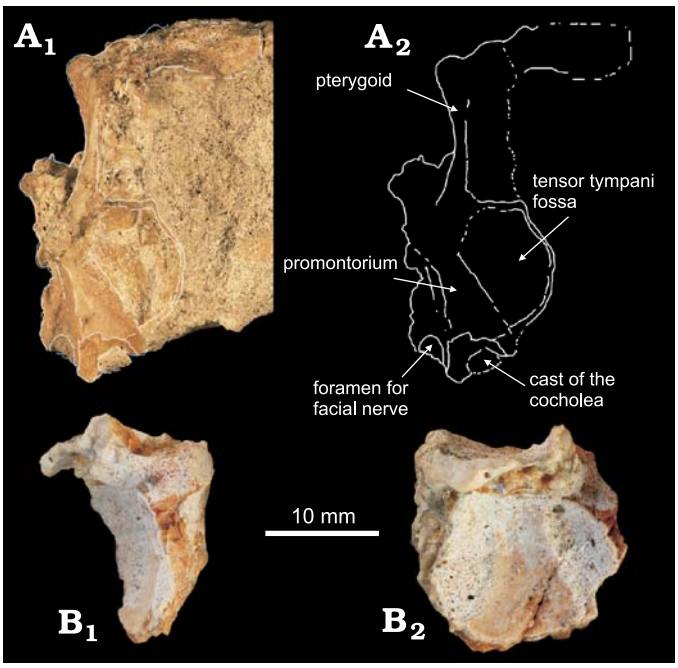

Fig. 10. Fragmentary pterygoid and middle ear cavity of multituberculate mammal *Sphenopsalis nobilis* Matthew, Granger, and Simpson, 1928 from the upper Paleocene Nomogen beds at the Erden (Urtyn) Obo locality, Inner Mongolia, China. **A**. IVPP V19025, middle ear with part of the promontorium in ventral view; photograph (A_1), explanatory drawing (A_2). **B**. IVPP V19029, possible bony shell of the inflated vestibule in lateral (B_1) and inside (B_2) views. The anterior end of each element is toward upside.

intertubercular groove is broad. In anterior (anteroventral) view (Fig. $11B_1$), the crest leading to the lesser tubercle is narrow, whereas the crest leading to the greater tubercle is broad. Distally, the deltopectoral crest is not preserved, but judging from the massive breakage at the base of the crest, it must be strong. The cross section of the mid-portion of the shaft has a triangular outline, which is considered characteristic of multituberculates (Kielan-Jaworowska and Qi 1990). Although incomplete, it is apparent that the distal end of the humerus is transversely wide. In anterior view (Fig. $11B_1$), the ulnar condyle is oval with the long axis parallel to the diaphysis; the condyle has a measurable maximum diameter of 10.4 mm. Although the distal part of the radial condyle is broken, it nonetheless appears globular and is slightly more proximally positioned than the ulnar condyle. The two condyles are separated by the intercondylar groove, which is more distinctive anteriorly than posteriorly. There is no trace of a trochlea. The entepicondyle is broken, but apparently projected strongly medially as reflected by its massive broken base. The entepicondylar foramen is small, with its posterior aperture at the dorsomedial edge of the thick entepicondyle, rather than at the posterior side of the bone (Fig. $11B_2$), similar to that in the recently described multituberculate humerus from the Late Cretaceous of Uzbekistan (Chester and Sargis 2010). Unlike many other multituberculates where the ectepicondyle is usually small, that in *Sphenopsalis*, although broken, is large. The ectepicondyle continues proximally as a wide crest on the lateral side of the distal humerus. In posterior (posterodorsal) view, the posterior crest is strong (Fig. $11B_2$). The shape of the broken radial condyle cannot be determined, but the ulnar condyle is prominent and is orientated diagonal to the long axis of the humerus. The maximum length and width of the ulnar condyle in posterior view are 13.3 mm and 8.4 mm, respectively.

Femur: Two incomplete femora are included in the present collection: a proximal part of a left femur, with the growth line of the epiphysis still visible, and a right femur with the proximal end missing. The incomplete femora were collected from the same pit and are here interpreted to be from the same individual (IVPP V19030; Fig. 12). Using the position of the post-trochanteric fossa and related landmarks on the two femora, the complete morphology and length of the femur can be reconstructed. The femur is stout, but in contrast to the humerus, the diaphysis is cylindrical, rather than triangular (Fig. 12). As in other multituberculates (Kielan-Jaworowska and Gambaryan 1994) and many therians, the femur has a nearly spherical head (maximum diameter of 14.3 mm) with an extensive articular surface, implying significant rotational capability at the hip. On the posteromedial side of the head is a small concavity, the fovea capitis, for the ligamentum teres. The neck is long and forms an angle of 50–60° with the greater trochanter, similar to many other multituberculates (Kielan-Jaworowska and Gambaryan 1994). The neck is rounded ventrally but is ridge-like on its dorsal border. The greater trochanter is robust and extends above the level of the head as in other multituberculates. In posterolateral view, the surface of the greater trochanter is pear-shaped, with a broad dorsal end that tapers ventrally. This area is commonly described as the rugose area of the greater trochanter in multituberculates (Kielan-Jaworowska and Gambaryan 1994; Kielan-Jaworowska et al. 2004), but in *Sphenopsalis*, it is smooth. The lesser trochanter is broken, but the breakage indicates that its long axis was parallel to the neck. A sharp ridge arising from near the breakage, presumably from the base of the lesser trochanter, runs distally for a short distance along the diaphysis. Lateral to the breakage is a shallow depression, the post-trochanteric fossa (Kielan-Jaworowska and Gambaryan 1994). The third trochanter is absent. A subtrochanteric tubercle, present in some multituberculates on the anterior side at the divergent point of the neck and the greater trochanter (Kielan-Jaworowska and Gambaryan 1994), is absent in *Sphenopsalis*.

The proximal end of the right femur is broken, but the post-trochanteric fossa and the ridge from the base of the lesser trochanter are preserved and mirror the structures on the proximal part of the left femur; as such, a nearly complete femur was reconstructed to have an estimated length of 86 mm. The diaphysis measures 11 × 8.7 mm in diameter at its proximodistal mid-point, but flares out toward the distal end, and measures 26.2 mm wide (transversely) and 15 mm long (anteroposteriorly). The epiphyseal line is distinct, and the distal condyles are massive. In anterior view, the lateral condyle is smaller and extends slightly more distally than the medial condyle. Unlike therians where the patellar

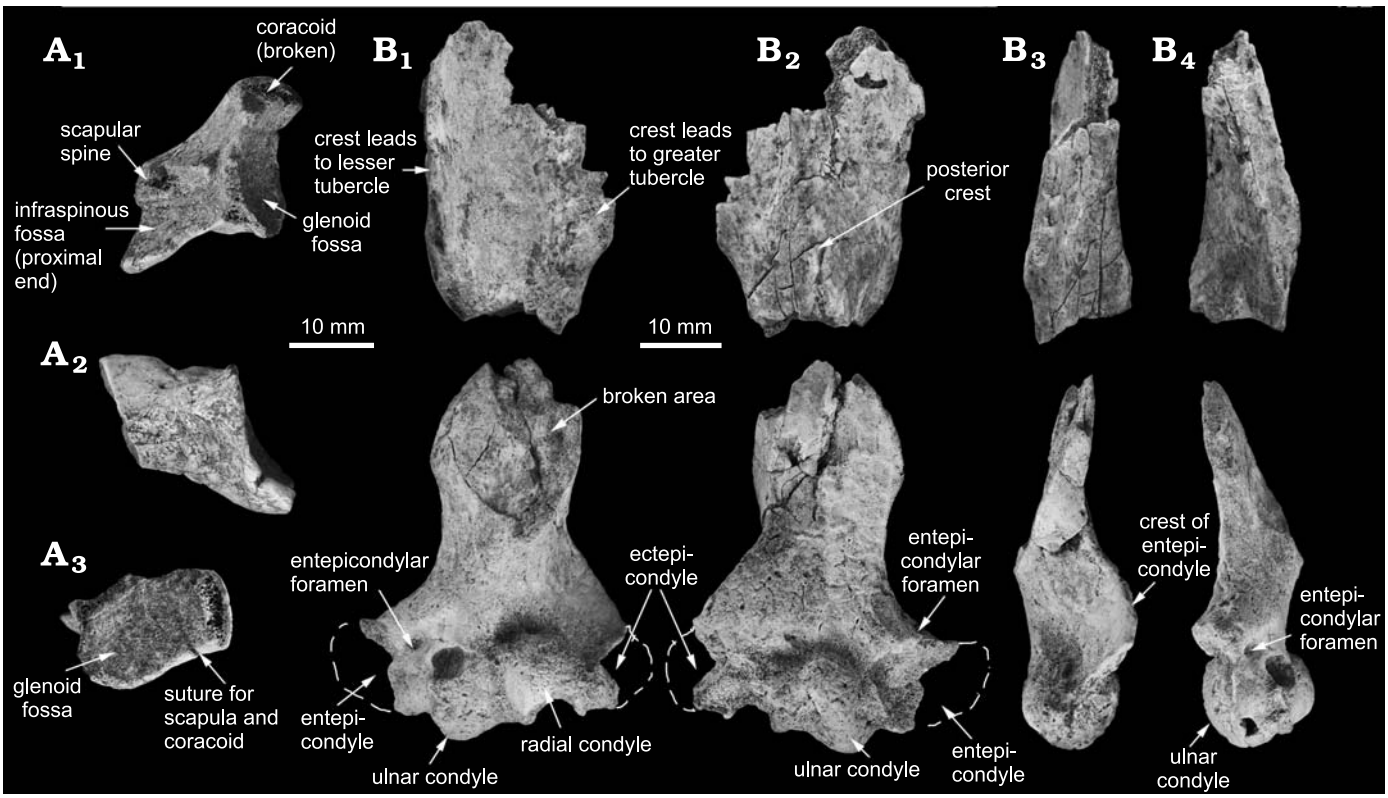

Fig. 11. Fragmentary scapula and humerus of multituberculate mammal *Sphenopsalis nobilis* Matthew, Granger, and Simpson, 1928 from the upper Paleocene Nomogen beds at the Erden (Urtyn) Obo locality, Inner Mongolia, China. **A**. IVPP V19030, proximal portion of the right scapula in lateral (A_1), medial (A_2), and ventral (glenoid fossa) (A_3) views. **B**. IVPP V19031, left humerus in anterior (B_1), posterior (B_2), lateral (B_3), and medial (B_4) views. Due to the breakage, the proximal (top) and distal (bottom) portions may not be displayed in their precise anatomical positions.

trochlea (groove) is well defined, long and symmetrical, the trochlea of *Sphenopsalis* is shallow and does not have a definitive shape. In posterior view, the lateral condyle is larger than the medial condyle. In distal view of the distal end of the femur, the medial condyle has an elongated oval shape, and the lateral condyle is more nearly spherical.

The right tibia (IVPP V19030) is nearly complete, with only the anterior side of the distal end being slightly crushed (Fig. 13). The diaphysis is somewhat distorted, but the length is 58.2 mm, and the diameter at the midpoint measures 8.8 mm mediolaterally and 7.5 mm anteroposteriorly. The mediolateral width of the proximal end is 26.6 mm, over twice the anteroposterior width, which measures 13 mm. In anterior or posterior view, the proximal end is strongly asymmetrical, owing to a large lateral process that extends laterally as a hook-like projection, with its tip pointing distally. In the proximal view, the articular surface of the tibial head consists of three areas, the first two consisting of an oval and smoothly concave articular facet for the medial condyle of the femur, and a transversely elongate articular facet for the lateral condyle of the femur; the former is more proximal (higher) than the latter, and the two facets are separated by the intercondylar eminence. In posterior view, the popliteal notch delimits the two facets. Anterior to the facet for the lateral condyle, there is a transverse groove, probably the extensor groove, which extends towards the lateral extremity of the head. Anterior to the extensor groove is the third area that has an irregular shape and does not seem to be part of the articular facet for the lateral condyle. In lateral view, the extensor groove makes a notch on the lateral edge of the proximal end of the tibia; the notch marks the route of the long digital extensor muscle in life. In posterior view, the edges of the two articular facets project posteriorly so that there is a large pocket on the posterior side of the proximal end of the tibia. On the posterolateral end of the lateral process is the facet for the fibula, which shows that the tibia and fibula are not fused and that the latter does not have a contact with the femur.

Remarks.—As mentioned above, "*Sphenopsalis noumugenensis*" was noted from the Nomogen Formation of Inner Mongolia (Jiang 1983), but this species has never been established through publication and should be considered a nomen nudum. Given the limited information from the type series of *S. nobilis*, as well as the variation we report on here (see below), there is no compelling evidence that the specimens from Urtyn Obo represent a different species. At present, we consider that the specimens collected from the Gashato Formation at Shabarakh Usu, Mongolia, and those reported here belong to the same species, and the morphological differences observed in these specimens represent individual variation within the species.

Comparisons.—*Lambdopsalis*: Among known multituberculates, *Sphenopsalis* is most similar to *Lambdopsalis* in

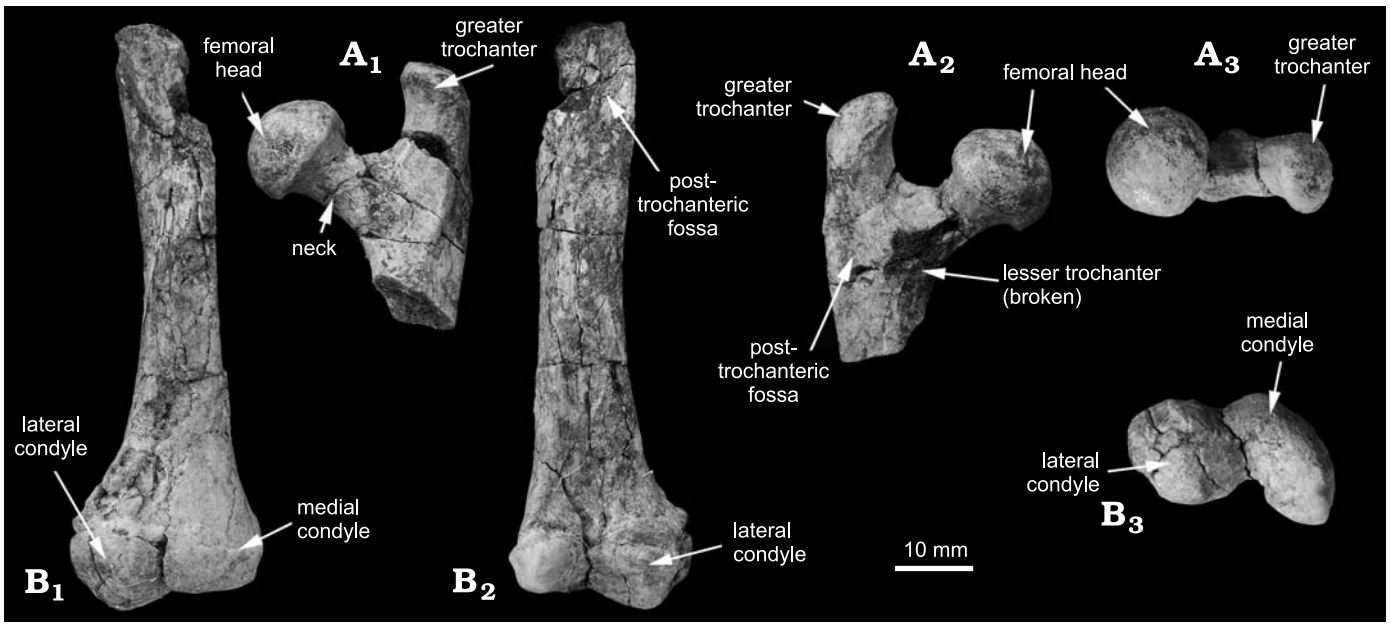

Fig. 12. The femur of multituberculate mammal *Sphenopsalis nobilis* Matthew, Granger, and Simpson, 1928 (IVPP V19030) from the upper Paleocene Nomogen beds at the Erden (Urtyn) Obo locality, Inner Mongolia, China. **A**. Proximal portion of the left femur in anterior (A_1), posterior (A_2), and proximal end (A_3) views. B. Right femur (with proximal end broken) in anterior (B_1), posterior (B_2), and distal end (B_3) views.

overall dental morphology (Miao 1986, 1988; Fig. 14). In both taxa, the enamel of M2 and m2 bear reddish pigmentation and the cusps are strongly crescentic, particularly those of the buccal row of M2 and the lingual row of m2. The I2 is not greatly enlarged in either genus, the crown is conical, tapering toward the tip, and the lower incisors are not transversely compressed. Furthermore, the central furrow of the upper molars is closed by a ridge that connects the mesial lingual and medial cusps, and in a reversed manner, a ridge connecting the distal lingual and buccal cusps closes the central furrow of lower molars distally. When Matthew et al. (1928: 3) described the partial m1 of *Sphenopsalis*, they recognized its smaller size in comparison with the M2; thus the authors noted: "it is not certain that this tooth belongs in this species". In light of the new specimens described in this study, it is clear that m1 is significantly narrower than m2 and M2, which is a feature shared by *Sphenopsalis* and *Lambdopsalis* (Figs. 7, 14) and reflects a occlusal pattern that differs from that of other taeniolabidoids (see Discussion).

As Miao (1986) noted, I3 of *Lambdopsalis* at the labial edge of the premaxilla is usually regarded to be plesiomorphic when compared with the general condition of mammals and early plagiaulacoid multituberculates, such as *Kuehneodon simpsoni* (Hahn, 1969) and *Psalodon fortis* (Simpson, 1929). Because in all the other Asian multituberculates where I3s are preserved in situ, they are situated on the palatal process close to the midline of the skull (Kielan-Jaworowska 1971, 1974; Kielan-Jaworowska and Dashzeveg 1978), Miao (1986) considered that the I3 position in *Lambdopsalis* is an apomorphic feature. As we show in this study, I3 of *Sphenopsalis* is not so reduced and is also marginally or buccally positioned, similar to that of *Lambdopsalis*. It seems that the marginal position of I3 is shared by *Lambdopsalis, Sphenopsalis*, and *Prionessus* (Meng et al. 1998; see below).

In describing the dentition of *Lambdopsalis*, Miao (1986) indicated that the buccal cusp row of m2 is only half as wide as the lingual row, contrasting with the nearly equivalent width of both cusp rows of m2 in *Prionessus* and *Sphenopsalis*. It is clear that both cusp rows of m2 in *Prionessus* are subequal, but the new specimens reported here show that *Sphenopsalis* has the same m2 condition of *Lambdopsalis*. When compared with the ultimate molars in other multituberculates (Kielan-Jaworowska et al. 2004), the m2 condition in which the lingual cusps are twice as wide as the buccal ones can be considered as another derived character shared by *Sphenopsalis* and *Lambdopsalis*. The M2s of both genera share a condition similar to that of m2, but in a reversed direction where the medial cusps are twice as wide as the lingual ones.

However, *Sphenopsalis* differs from *Lambdopsalis* in being significantly larger. Although I3 position is similar to that of *Lambdopsalis,* but minor differences exist. For instance the I3 is much smaller than I2, compared to those of *Sphenopsalis,* and slightly distolingual to I2 in *Lambdopsalis* (Miao 1986, 1988; F-YM and JM personal observation). Miao (1986) recognized that *Lambdopsalis* differs from *Prionessus* and *Sphenopsalis* in having its sharper posterior end of m1 wedged between first cusp apices of buccal and lingual rows of m2. The m1 of *Sphenopsalis* does not seem to have such a sharp distal projection, although its distal end does project distally and indent the mesial surface of m2 (Fig. 7).

Cusps of M1 and m1 of *Lambdopsalis* are all crescentic at a greater degree than those of *Sphenopsalis* (Fig. 14). In *Sphenopsalis* the lingual side of the medial cusps of M1 has only a short ridge and the cusps show a rectangular outline after wear instead of being distinctively crescent. Cusps

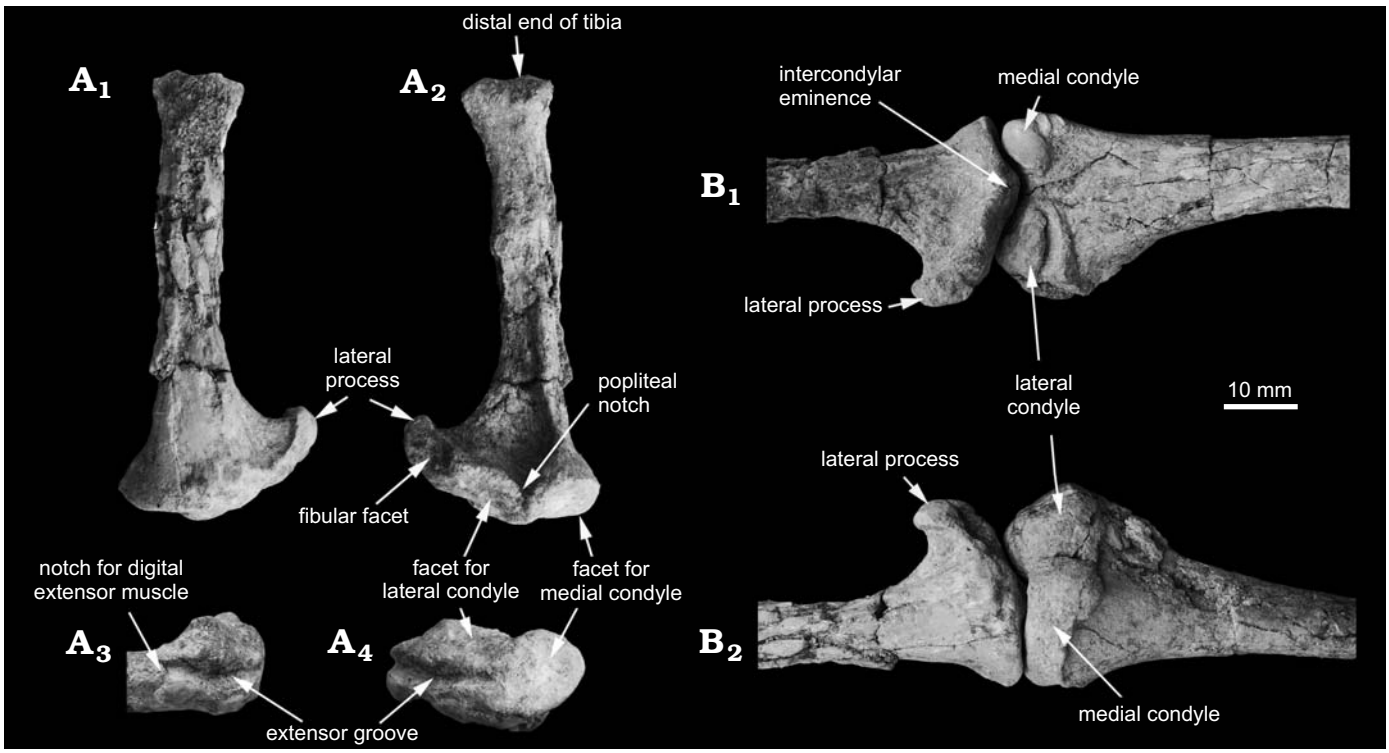

Fig. 13. The tibia of multituberculate mammal *Sphenopsalis nobilis* Matthew, Granger, and Simpson, 1928 (IVPP V19030) from the upper Paleocene Nomogen beds at the Erden (Urtyn) Obo locality, Inner Mongolia, China. **A**. Right tibia in anterior (A_1) and posterior (A_2) views, proximal end in lateral (A_3) and proximal (A_4) views. **B**. Femur-tibia articulation in posterior (B_1) and anterior (B_2) views.

on both rows of m1 have long ridges that extend distally in *Lambdopsalis*, in contrasting the relatively short ridges in *Sphenopsalis* (Fig. 7). The M2 and m2 in *Sphenopsalis* are more crescent than M1 and m2, respectively, but their ridges are not so sharp as those of *Lambdopsalis* (Fig. 14).

Cranial features of *Sphenopsalis* are still poorly known compared to *Lambdopsalis* (Miao 1988). The incisive foramen of *Sphenopsalis* is proportionally much larger than that of *Lambdopsalis,* which is certainly a unique and peculiar feature of *Sphenopsalis*. Again, if the structure we interpreted as the inflated vestibule for *Sphenopsalis* is correct, it will be a cranial feature shared by *Sphenopsalis* and *Lambdopsalis*. Other aspects of the middle ear cavity of *Sphenopsalis* are significantly different from that of *Lambdopsalis*. For instance*, Lambdopsalis* does not have a broad tensor tympani fossa (Miao 1988; Meng and Wyss 1995) and the promontorium of *Sphenopsalis* is different from that of *Lambdopsalis*; the latter is finger-like shaped (Miao 1988; Meng and Wyss 1995; F-YM and JM personal observation).

One cranial character that is unclear is the contribution of the frontal to the orbital rim. It is one of the diagnostic features for Taeniolabidoidea that the frontal is small, pointed posteriorly, and almost or completely excluded from the orbital rim (Kielan-Jaworowska and Hurum 2001; Kielan-Jaworowska et al. 2004). This is the condition of *Sphenopsalis* as we interpreted from the fragmentary skull. However, *Lambdopsalis*, a member of Taeniolabidoidea, has a narrow frontal contribution to the orbital rim, on which there is a postorbital process (Miao 1988). The narrow part of the frontal is separated from the main portion of the frontal on the skull roof by the nasal-parietal connection. This configuration indicates that the nasal-parietal must have overlapped a significant part of the frontal in *Lambdopsalis*. In this regard, *Sphenopsalis* differs from *Lambdopsalis*.

When Kielan-Jaworowska and Qi (1990) described some postcranial elements from *Lambdopsalis*, they were not sure whether those are from *Lambdopsalis*, *Sphenopsalis*, or even *Prionessus*. With the new specimens reported here, it is clear that those described by Kielan-Jaworowska and Qi (1990) were not from *Sphenopsalis* or *Prionessus*. It is most likely from *Lambdopsalis,* which is supported by our observations of numerous postcranial specimens of *Lambdopsalis* collected in recent years. All these postcranial elements cannot be from *Prionessus* because they are too large for *Prionessus*. Kielan-Jaworowska and Qi (1990) considered the humeri they described were possibly the stoutest ones within multituberculates at the time. The new materials of *Sphenopsalis* are certainly much more robust, both in absolute and relative size, than that of *Lambdopsalis*. Although the forelimbs are robust in both taxa, which perhaps suggest fossorial life, their incisors are relatively small, much weaker than those of the North American taeniolabidoids and unlike typical fossorial mammals that use teeth for burrowing.

To sum up, the dental, cranial and postcranial show that *Sphenopsalis* and *Lambdopsalis* are two distinctive taxa and yet, they share many features that strongly indicate a close relationship. The similar morphological features suggest similar adaptation and life styles. However, because they co-existed

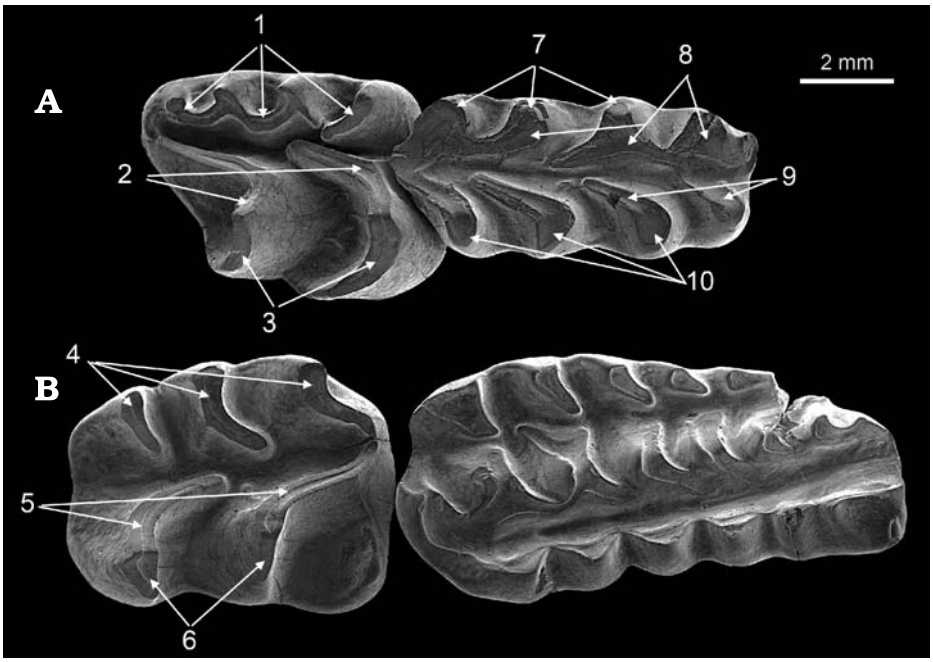

Fig. 14. The upper and lower left molars of multituberculate mammal *Lambdopsalis bulla* Matthew, Granger, and Simpson, 1928 (IVPP V20101) from the upper Paleocene Nomogen beds at the Bayan Ulan locality, Inner Mongolia, China. Crown view of m1–2 (**A**) and M1–2 (**B**). Wear facets: 1, on lingual sides of the buccal cusps of m2; 2, on buccal sides of the lingual cusps of m2; 3, on lingual sides of the lingual cusps of m2; 4, on buccal sides of the lingual cusps of M2; 5, on lingual sides of medial cusps of M2; 6, on the buccal sides of medial cusps of M2; 7, on buccal sides of the buccal cusps of m1; 8, on lingual sides of the buccal cusps of m1; 9, on buccal sides of the lingual cusps of m1; 10, on lingual sides of the lingual cusps of m1; no wear facet was developed yet on the cusp of the buccal (external) cusp row of M2 in this specimen.

in the same fauna, one may assume that they had differentiated ecological niches when they existed sympatrically. Their phylogenetic relationship will be further discussed below.

Prionessus: *Prionessus lucifer* (Matthew and Granger, 1925) was named on the basis of an edentulous mandible (AMNH 20423). As noted by Meng et al. (1998), several additional specimens that were collected in 1925 were not described, including a lower jaw with p4, m1 and erupting m2 (AMNH 21731), which was designated as the topotype. In reporting additional specimens of *Prionessus* from the Bayan Ulan locality, Inner Mongolia, Meng et al. (1998) revised the diagnosis of *Prionessus*. *Prionessus* is similar to *Sphenopsalis* in having a lower incisor that is oval in cross section, with enamel covering the labial side of the tooth; in having a conical I2 with the enamel restricted to the labial side; in having a relatively simple I3 that is positioned at the labial margin of the palate, lateral to the posterior end of the elongate, medium sized incisive foramen; and in P4 being single-cusped and having one or two roots.

The main features that distinguish *Prionessus* from *Sphenopsalis* include: much smaller in body size; cusp formula for m1–2 and M1–2 being 5:4, 3:2 or 4:2, 6–7:7–8:4–5 and 1:2:3, respectively; I3 proportionally much more reduced than I2; p4 at least in some specimens having two roots; molar cusps conical and with weak crests; the lingual and buccal cusp rows of m2 subequal in width. Simmons (1993) recognized several features of *Prionessus* that she considered more primitive than those of *Lambdopsalis* and *Sphenopsalis*, including fewer cusps on M1, the posterior border of the palate occurring medial to the midpoint of M2, and the nasal not contacting theparietal. The last two features are presently unknown in *Sphenopsalis*.

In general, the molar morphology of *Prionessus* is more similar to those of the Late Cretaceous multituberculates from Mongolia (Kielan-Jaworowska et al. 2004) and represented a relatively primitive form of taeniolabidoids. The most distinctive features shared by these three taeniolabidoids are the simple incisors with I3 positioned at the labial margin of the palate and the small, simplified and only P4/p4.

Taeniolabis: *Sphenopsalis nobilis* from the late Paleocene is by far the largest known multituberculate in Eurasia, whereas *Taeniolabis taoensis* from the early Paleocene is the largest known multituberculate (Cope 1882; Granger and Simpson 1929; Simmons 1987; Wilson et al. 2012). When the teeth of the two species are compared, *T. taoensis* is considerably larger than *S. nobilis* and has a distinctively different cusp arrangement and morphology (Fig. 15). In revising the diagnosis for *Taeniolabis*, Simmons (1987) emphasized the greater dimensions of i1, I2, and M2/m2, the cusp formula and the ratio of P4/M1. The new specimens of *Sphenopsalis* show that cusp formula and P4/M1 length ratio may not adequately distinguish *Taeniolabis* and *Sphenopsalis*, but incisor size and shape differ significantly between the two genera. The upper incisors, particularly I2, of *Sphenopsalis* are proportionally much smaller than the beaver-like incisors of *Taeniolabis*, which has a well-defined and thick enamel band on the labial (anterior) side of I2. Other major differences between these two taxa are the molar size proportions and cusp shapes. Compared to *Taeniolabis*, the M1 crown of *Sphenopsalis* is low and cusps are slim (not so inflated), but both taxa show deepest wear at the distal part of M1. The major dental differences for *Taeniolabis* and *Sphenopsalis* are between their M2/m2s. The M2/m2 of *Sphenopsalis* are highly crested, forming strong and sharp cutting edges appropriate for shearing, whereas those of *Taeniolabis* are heavy and quadrangular, suggesting the use in grinding (Fig. 15).

Taeniolabis and *Sphenopsalis* were two of at least five genera previously placed in the family Taeniolabididae (Taeniolabidoidea) (Fox 1999, 2005; Kielan-Jaworowska and Hurum 2001; Kielan-Jaworowska et al. 2004). The main den-

tal features that shared by them include the follows: only one upper premolar, a long diastema between I3 and the premolar, the premolar strongly reduced in proportion to enlarged upper and lower multicusped molars, M1 with three rows of cusps with lingual one extending for the entire length of the tooth (Kielan-Jaworowska and Hurum 2001). Some of these features, such as the size of P4 and morphologies of M1 and m2, are unknown for *Sphenopsalis* until this study. One of the diagnostic features for Taeniolabidoidea, sharing with most Djadochtatherioidea and Eucosmodontidae, is a strong, self-sharpening incisor with limited enamel band (Kielan-Jaworowska and Hurum 2001; Kielan-Jaworowska et al. 2004). This feature was originally used to define Taeniolabidoidea (Sloan and Van Valen 1965). However, the self-sharpening incisors are not developed in *Sphenopsalis,* nor are in *Lambdopsalis* and *Prionessus*, as discussed above. In addition to the limited enamel band on the incisor, incisor self-sharpening requires several other features, as best shown in Glires, such as *Rhombomylus* (Meng et al. 2003). The enlarged upper and lower incisors are strong and generally chisel-like and have a cutting edge formed by the enamel layer at the tooth tip, as in *Taeniolabis* (Granger and Simpson 1929) and *Catopsalis* (Middleton 1982). To create and maintain the cutting edge, the lower jaw must be able to move forward and backward, and the upper and lower incisors can constantly hone each other on the distal surface (the dentine part) of the incisor tip. This further implies that the incisors are evergrowing, although the enamel deposition ceased at a stage of ontogeny during the life of the animal, as in *Taeniolabis* (Granger and Simpson 1929). As we show above (Fig. 3), except for the enamel band, the upper incisor of *Sphenopsalis* has a circular cross-section and does not have the cutting edge at the tip; the closely packed I2 and I3 actually prevent such a cutting function. The similar condition is present in *Lambdopsalis* (Miao 1986, 1988) and *Prionessus* (Meng et al. 1998; F-YM and JM personal observations).

The similar comparison can be made between *Sphenopsalis* and *Catopsalis*, which is smaller than *Taeniolabis* but has a similar tooth pattern (Granger and Simpson 1929; Middleton 1982; Lucas et al. 1997). Its relationship to *Taeniolabis* is perhaps analogous to that of *Lambdopsalis* to *Sphenopsalis*.

Stratigraphic and geographic range.—The late Paleocene Gashato Formation at Shabarakh Usu, Mongolia (the type horizon and locality). The Nomogen Formation at the Erden (Urtyn) Obo locality (also named as Aliwusu on the topographic map) (this study) and possibly the Haliut locality (Chow and Qi 1978) in the Nomogen district, Inner Mongolia; the late Paleocene Gashatan land mammal age.

Phylogenetic analyses

In addition to the morphological comparisons that show the similarities and differences between *Lambdopsalis* and *Sphenopsalis* and differentiate them from other taeniolabidoids, we also conducted phylogenetic analyses that focus on the placement of *Sphenopsalis* and test the relationships of *Lambdopsalis* and *Sphenopsalis* with other multituberculates. The primary data matrix we adopted for the purpose is from Yuan et al. (2013), which was built up from several studies (see Material and methods). We do not intend to review all the taxa (genera) and characters that were used in the previous studies, which is beyond the scope of this study. However, we did modify some character coding for taxa where additional morphological evidence is available, as we specified in the character list in the SOM 2. Except for removing the hypothetic ancestor from the data matrix used by Yuan et al. (2013), we added three taxa, *Sphenopsalis*, *Prionessus* and *Catopsalis*, to the data matrix. These are three taeniolabidoid taxa that are relevant to this study.

Fig. 15. Teeth of multituberculate mammal from the lower Paleocene Puercan in the San Juan Basin, New Mexico. **A**. *Taeniolabis* sp., AMNH 117415, cast, occlusal view of right p4–m2. **B**, **C**. *Taeniolabis taoensis* Cope, 1882. **B**. AMNH 16310, occlusal view of the left p4–m2. **C**. AMNH 16321, occlusal view of the right P4–M2.

Because many multituberculate species were based on fragmentary material, the terminal taxa used for phylogenetic analyses of multituberculates have to be at the generic level (Simmons 1993; Rougier et al. 1997; Kielan-Jaworowska and Hurum 2001; Yuan et al. 2013). Among those terminal taxa, some genera are monotypic, such as *Sphenopsalis*, *Prionessus*, and *Lambdopsalis*, and others contain more than one species, such as *Taeniolabis* and *Catopsalis*. For the latter, it has not been specified which species were scored for each genus in previous studies. Given the focus of our phylogenetic analyses, we directly adopted the coding of the genera from previous studies (Simmons 1993; Rougier et al. 1997; Kielan-Jaworowska and Hurum 2001; Yuan et al. 2013) except for *Sphenopsalis* and *Prionessus,* which were not used in those phylogenetic analyses. Some character codings used by Yuan et al. (2013) were modified for a few genera and the sources and reason for the modifications are given in character list (SOM 2).

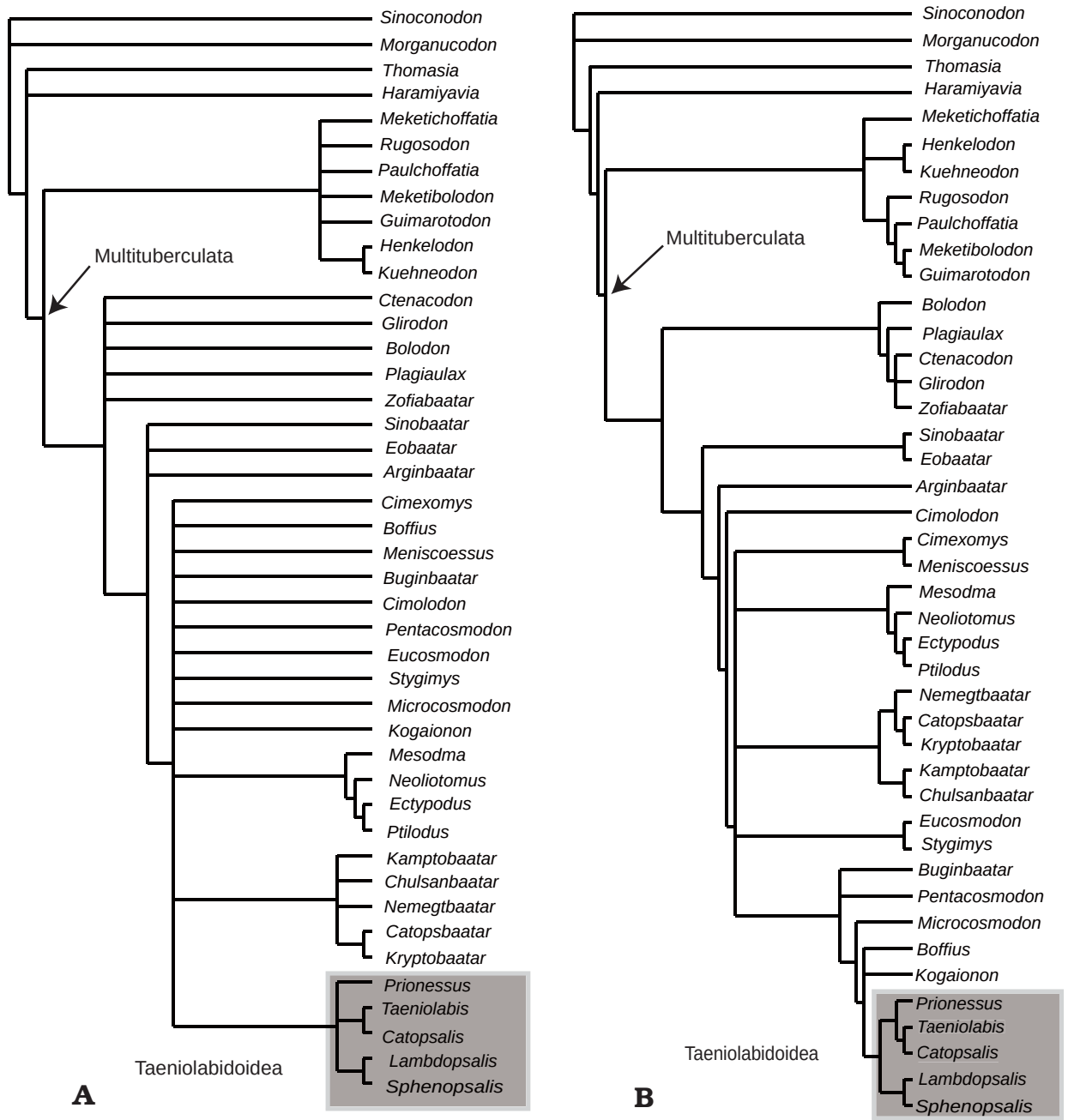

Fig. 16. Phylogenetic position of *Sphenopsalis nobilis* within multituberculates. **A**. The strict consensus tree of 70 most parsimonious trees obtained in the PAUP search where all characters were unordered. **B**. The 50% majority rule consensus tree with all characters unordered. See additional supporting data in the SOM.

The phylogenetic analyses were performed using PAUP (Swofford 2002) with a heuristic search criterion. The search settings for the preferred tree (Fig. 16A) are as the following: The optimality criterion is parsimony. All characters are unordered and equally weighted; multistate taxa are interpreted as polymorphism. Gaps are treated as "missing" and multistate taxa interpreted as polymorphism. A random stepwise addition sequence was used with 1000 replicates. Of the 102 characters, two are parsimony-uninformative. Number of trees held at each step during stepwise addition is 10 and the branch-swapping algorithm is tree-bisection-reconnection (TBR). Figure 16 presents the strict and 50% majority rule consensus trees resulted from 70 trees retained in the search. The tree length of the strict consensus is 387; the consistency index (CI) is 0.4083; the homoplasy index (HI) is 0.5917; the retention index (RI) is 0.6963; the rescaled consistency index (RC) is 0.2843.

We also conducted PAUP searches with 19 characters being ordered (see SOM 2), following Yuan et al. (2013). Other search settings are the same as those described above. The strict and 50% majority rule consensus trees resulted from 10 trees retained in the search are presented in Fig. 17. The data matrix, the character list and the PAUP logs for all the four trees are provided in the SOM 3 and 4. Given that the focus of

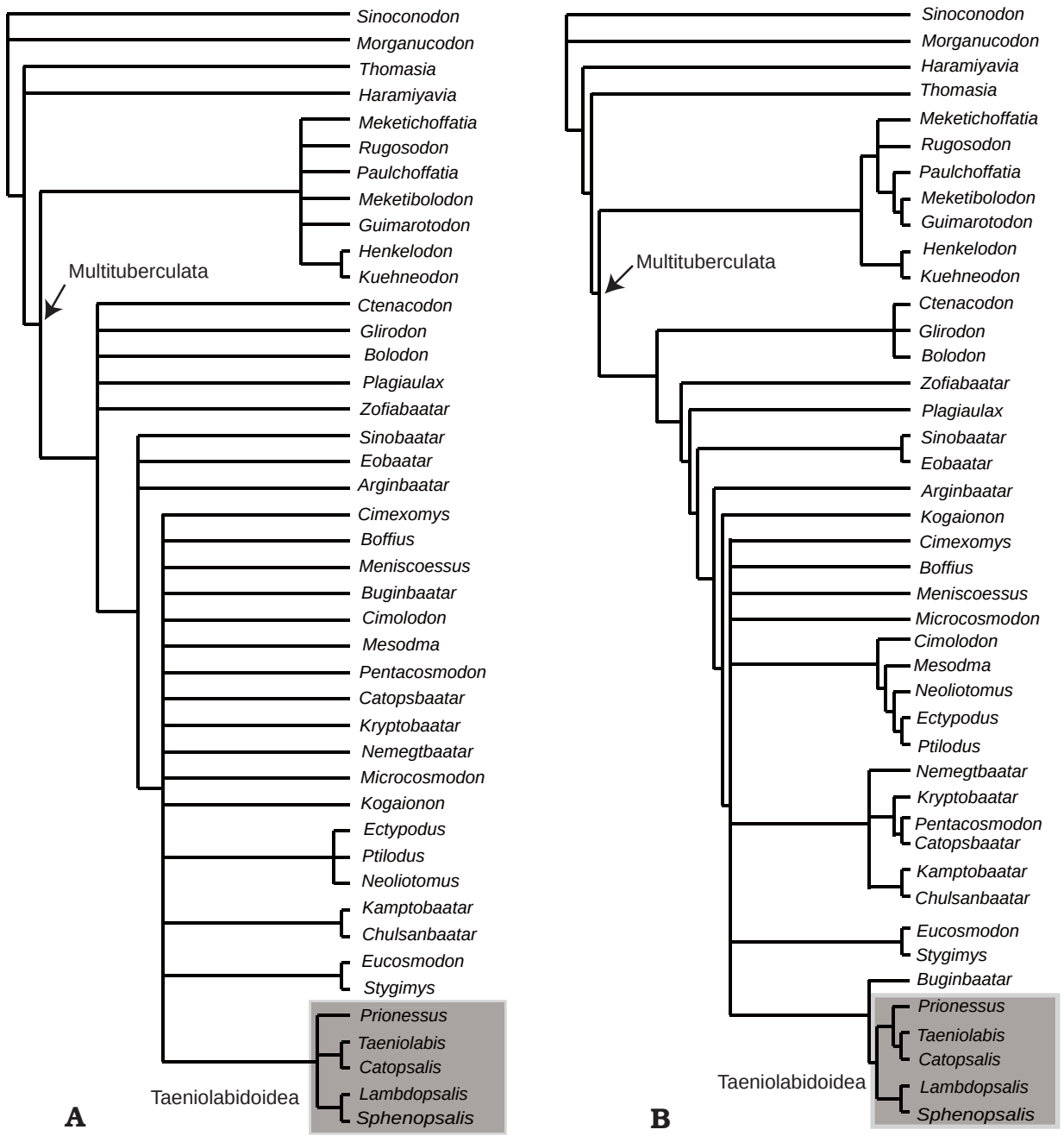

Fig. 17. Phylogenetic position of *Sphenopsalis nobilis* within multituberculates. **A**. The strict consensus tree of 138 trees obtained in the PAUP search where 19 characters were ordered (see SOM). **B**. The 50% majority rule consensus tree with 19 characters ordered. See additional supporting data in the SOM.

this study is on the phylogenetic relationships of *Sphenopsalis* within Taeniolabidoidea and the assessment for the relationship between North American and Asian taeniolabidoids, our discussion below will concentrate on these groups.

Discussion

Phylogeny and taxonomy.—*Sphenopsalis* was regarded as "a very peculiar form and quite different from any other known multituberculate" by Granger and Simpson (1929: 665) at the time when only a few Paleogene multituberculates were available for comparison. The report of *Lambdopsalis*, on which a monotypic family Lambdopsalidae was proposed (Chow and Qi 1978), further complicated the situation. Immediately after publication of *Lambdopsalis,* Kielan-Jaworowska and Sloan (1979: 195) commented: "It cannot be also excluded that *Lambdopsalis* is a junior synonym of *Sphenopsalis* but the decision is left to the authors of *Lambdopsalis*." This view was not followed thereafter, and subsequent to the studies by Miao (1986, 1988), *Lambdopsalis* has been generally accepted as a valid genus (e.g., Simmons 1993; Rougier et al. 1997; Kielan-Jaworowska et al. 2004; Wilson et al. 2012). The peculiarity of *Sphenopsalis* has persisted, however, be-

cause no additional material had been reported since its initial discovery and description. Miao (1986: 75) pointed out: "Unfortunately, teeth anterior to the molars of *Sphenopsalis* have not been found, and the affinity of *Sphenopsalis* relative to *Prionessus* and *Lambdopsalis* must be established solely on synapomorphic characters of molars." In fact, in addition to teeth anterior to the molars, the M1 of *Sphenopsalis* was unknown, and the lower molars were known only from fragments. However, the isolated teeth of *Sphenopsalis* already exhibited sufficient information that let Granger and Simpson (1929: 665) note that "*Sphenopsalis* and *Taeniolabis*, indeed, represent opposite extremes of adaptation, and their wider systematic separation may be necessary when the former is better known". Because of the sparse specimens, Miao (1986: 74) recognized that "considering limitations of morphological knowledge of *Prionessus* and *Sphenopsalis* plus the poor understanding of phylogenetic interrelationships of Asian taeniolabidoids, it is premature to make judgments on the validity of Lambdopsalidae". In a later study on the cranial morphology of *Lambdopsalis*, Miao (1988: 94) concluded that: "Lambdopsalidae Chow and Qi, 1978 was established as a monotypic family solely on the basis of the supposed presence of tympanic bulla in *Lambdopsalis*. In light of new information of cranial morphology (this study) and from the dental anatomy (Miao, 1986), *Lambdopsalis* is referred to Taeniolabididae Granger and Simpson, 1929. I consider Lambdopsalidae to be invalid, a subjective junior synonym of Taeniolabididae".

As recognized by Miao (1988), the main reason that Lambdopsalidae was proposed was because the vestibular apparatus in *Lambdopsalis* was mistakenly identified as an inflated tympanic bulla, "a character which is quite unique and renders it difficult to affiliate it to any known multituberculate group" (Chow and Qi 1978: 85). Later studies showed that a relatively inflated vestibule was not uncommon among Cretaceous and Paleogene multituberculates (Luo and Ketten 1991; Fox and Meng 1997; Hurum 1998), but none of them shows the degree of inflation as in *Lambdopsalis* (Chow and Qi 1978; Miao 1988; Meng and Wyss 1995) and in *Sphenopsalis*, if our identification of the vestibule in this study is correct. Miao (1988: 89) argued that "most dental and cranial characters show phylogenetic unity of *Lambdopsalis* with the other taeniolabidid genera", but this argument was made without sufficient evidence from *Sphenopsalis*. We show in this study, listed in the diagnosis for the family and discussed in the text, *Lambdopsalis* and *Sphenopsalis* are dentally and probably cranially more similar to each other than either to any other multituberculate.

Since Matthew et al. (1928), the close relationship among *Sphenopsalis, Prionessus*, *Catopsalis*, and *Taeniolabis* and their distinction from ptilodontids have been recognized (Miao 1986, 1988). However, there were few phylogenetic analyses that included *Lambdopsalis*, *Prionessus*, and *Sphenopsalis*, partly because of the sparse specimens of *Prionessus* and *Sphenopsalis*. The analysis by Simmons and Miao (1986) (see also Simmons 1987) recognized the three taxa as a monophyletic group, which may form a sister group of *Taeniolabis*, probably plus *Catopsalis,* although *Catopsalis* was considered as a non-monophyletic taxon. In the analysis by Simmons and Miao (1986), *Lambdopsalis* and *Prionessus* form a sister-group that pairs with *Sphenopsalis.*

For the first time, our phylogenetic analyses include the five genera traditionally placed within Taeniolabidoidea. The results show that the resolution of the tree topology is better when some of the characters were ordered (Fig. 17). However, in all analyses, either with all characters unordered or with some ordered, Taeneolabidoidea as a monophyletic group was identified. Within Taeneolabidoidea, the Asian *Lambdopsalis–Sphenopsalis* clade and the North American *Taeniolabis–Catopsalis* clade are stable in all analyses. These topologies reflect many derived features shared by the *Lambdopsalis–Sphenopsalis* clade on the one hand and the *Taeniolabis–Catopsalis* clade on the other, as we discussed above. *Prionessus* is the taxon that has a relatively unstable placement within taeniolabidoids. In three of the four consensus trees (Figs. 16B, 17), *Prionessus* is at the base of the *Taeniolabis–Catopsalis* clade, but in the strict consensus tree with all characters unordered (Fig. 16A), *Prionessus* and the other two clades form a polytomy. When reporting *Prionessus* and *Sphenopsalis,* Matthew et al. (1928: 4) noted that "In the American form the cusps have apparently become heavier and more quadrate, in the Mongolian more compressed and crested, but it is a tenable hypothesis that these represent divergent adaptations from a more or less intermediate ancestral type, perhaps more nearly preserved in the Mongolian *Prionessus* and, probably to less extent, in the American *Catopsalis*." The more general morphology of *Prionessus* probably represents the primitive condition for taeniolabidoids, but the current evidence is not sufficient to conclusively support *Prionessus* as an "intermediate ancestral type" for taeniolabidoids.

For the least resolved tree (Fig. 16A), characters supporting Taeniolabidoidea are many, of which those with the consistency index equal or greater than 0.5 include at least the following: no large diastema between the second and third upper incisors, I3 single cusped or peg-like, I3 on the margin of the premaxilla, one upper premolar, the premolar single-rooted, one main cusp row on P4, lower p4 not laterally compressed to be bladelike, p4 crown profile triangular in lateral view, M1 lingual row cusp count 7–9 or more, and the frontal deeply inserted between the nasals. In the same consensus tree (Fig. 16A), characters (CI $\geq$ 0.5) that support Taeniolabididae (the *Taeniolabis–Catopsalis* clade) include: P4 with one main row and a shorter buccal row, M2 with uniform valley that is anteriorly open, the middle valley of M1 indistinctive owing to inflation of tooth cusps, M2 middle valley absent due to inflation of tooth cusps, and teeth with inflated cusps. Characters (CI $\geq$ 0.5) that support Lambdopsalidae (the *Lambdopsalis–Sphenopsalis* clade) include: the central valley of lower molars closed distally by a narrow crest closes the narrow, the m1 middle valley present and rimmed and projected distally, the m2 middle valley present and closed distally by a ridge,

the m2 labial cusp row longer than the lingual row and tooth cusps in crescentic shape.

In addition to the characters that were used in the current data matrix, we think several characters that diagnose Lambdopsalidae could be used in future phylogenetic analyses and will most likely support the *Lambdopsalis*–*Sphenopsalis* pairing. These include such characters as that the width of the lingual cusp row of m2 is twice of the buccal one, the width of the medial cusp row of M2 is twice of the lingual one, and the m1 is significantly narrower than m2. Furthermore, the M1/M2 and m1/m2 length ratio may also be informative to distinguish Taeniolabididae from Lambdopsalidae. Characters supporting the relevant nodes in other trees are provided in the SOM 2. In general, we prefer the result of Fig. 16A because we do not assume evolutionary transformation of a character a priori.

With the new evidence of *Sphenopsalis*, it is clear that *Lambdopsalis* and *Sphenopsalis* are both valid genera, which supports the conclusion reached by Miao (1986, 1988) on the taxonomic status of *Lambdopsalis*. These two taxa differ from each other in numerous aspects and each retains its own autapomorphies, as we compared in the previous sections. On the other hand, as Chow and Qi (1978) noted the dental similarity between *Lambdopsalis* and *Sphenopsalis,* our study further shows that the two Asian forms are most similar to each other than either of them to any other multituberculates. Our conclusion supports Granger and Simpson's (1929) observation that a major evolutionary dichotomy probably existed within taeniolabidoids. We think that the morphological evidence and phylogenetic relationship presented in this study justify our proposal to re-establish the family Lambdopsalidae Chow and Qi, 1978. This family represents its own evolutionary direction that is different from that of the North American taeniolabidids.

Occlusal pattern.—In a recent study on multituberculate tooth morphologies and their ecological implications, Wilson et al. (2012) showed that disparity in dental complexity rose with generic richness and disparity in body size across the Cretaceous–Paleogene (K–Pg) transition and that an adaptive shift towards increased herbivory was little affected by the K–Pg mass extinction. The study did not include *Sphenopsalis* because of its poor fossil record. The new evidence that we present here on the tooth morphology and body size of *Sphenopsalis* lends additional support to the hypothesis of Wilson et al. (2012). Kielan-Jaworowska et al. (2004: 279) recognized that, because of development of an additional cusp row on the upper molars, the upper and lower teeth in cimolodontans are "as a rule more horizontally worn, and the wear facets face upward on the lower molars and downward on the uppers". This is unquestionably applicable to the Taeniolabididae within Taeniolabidoidea, particularly for teeth with considerable wear, but not to Lambdopsalidae, even though the extra cusp row was developed on the upper molars of lambdopsalids. As early as in the study where *Sphenopsalis* was named, Matthew et al. (1928: 4) already recognized that "The dentition, so far as revealed, is certainly multituberculate but of an adaptive type very different from that of any other known genus. The high, narrow, sharp crests of the cusps are little fitted for heavy crushing or grinding but form a cutting device of remarkable perfection, probably an adaptation to some specific type of vegetable food." The same statement is also applicable to *Lambdopsalis* that was discovered 50 years later (Chow and Qi 1978). Specifically, wear facets are formed on the two buccal and lingual slopes of the medial cusps on the upper molars (Figs. 4, 5, 7, 14), which make the cusp in a triangular shape in distal view. Compared to other taeniolabidoids, the crests or ridges of the medial cusps are long and sharp in lambdopsalids. The m1 is narrow and wear facets are on both sides of the lingual and buccal cusps (Fig. 14). This indicates that the medial cusp row of M1 bites in the central furrow of m1, where the lingual and buccal rows of m1 bite into the lingual and buccal furrows of M1, respectively. The M2/m2 occlusal pattern is similar in *Lambdopsalis* and *Sphenopsalis* in having the medial cusp row of M2 occludes with the central valley of m2 (or the lingual cusp row of m2 bites into the valley in M2). The central valley in either M2 or m2 is broadly V-shaped in distal view and the wear facets are not horizontal unless the teeth were deeply worn in very old individuals (Fig. 8G).

Although it has been known that the occlusal patterns in M1/m1 and M2/m2 are different in multituberculates (Van Valen 1976; Krause and Hahn 1990; Kielan-Jaworowska et al. 2004), the difference seems not always clearly expressed. As a general example, only the occlusal pattern of M1/m1 of multituberculates was discussed when "Occlusion" of multituberculates was introduced in Kielan-Jaworowska et al. (2004: 279). As a specific example, in describing the M2 of *Lambdopsalis* Miao (1986: 70) wrote: "Wear facets develop on both sides of the medial cusps, the medial side of the internal cusps, and the labial side of the external cusp…. Wear facets on the medial sides of the internal cusps are ridge-like, and extend anteromedially." In the context of the description of Miao (1986: 70) "wear facets on the medial sides of the internal cusps" appears to mean lingual sides of the internal cusps of M2, which, if so, is incorrect. There should be no wear facet on lingual sides of the lingual cusps of M2 in multituberculates (Fig. 14). This is because the M2 is positioned one cusp row lingual to M1 so that the lingual cusps of m2 occlude in the valley of M2 in chewing and the lingual sides of the lingual cusps of M2 are not engaged in any grinding or shearing contact with the lower molar.

We emphasize the occlusal pattern here because lambdopsalids display clear wear facets on the molars that show the relationships of the primary and secondary cusps, which are critical to understand the evolution of the allotherian tooth pattern. The M2/m2 occlusal pattern was recognized as to be suggestive for relationships between multituberculates and haramiyidans (Van Valen 1976), which gains support from several recent studies on newly discovered haramiyidans (Zheng et al. 2013; Bi et al. 2014; Meng et al. 2014;

Meng 2014). In light of the new material of haramiyidans and multituberculates, the occlusal pattern within multituberculates needs to be re-considered. One of the issues concerns the homology (at least semantically) of the cusp row of the M2 in multituberculates. In paulchoffatiines, it is the buccal cusp row of M2 that was considered in continuity with the lingual row of M1 and occluded in the valley of m2 (Krause and Hahn 1990), but in lambdopsalids, it is the medial cusp row, perhaps with the contribution of the buccal (external) cusp of M2, that occludes in the valley of m2. This raises the issue about the homology of the cusp rows in multituberculates. A brief discussion on the homology of the cusp rows in allotherians has been proposed by Meng (2014), but a more detailed treatment, particularly in association with more advanced multituberculates, is needed.

In addition to the cusp wear facets, the tooth shape and size are also suggestive for the occlusal pattern of lambdopsalids and taeniolabidids. In comparison, the mean length/width of M1–2 for *Taeniolabis taoensis* are 23/11.6 and 14.4 /12 mm (Simmons 1987) and the same dimensions for *Sphenopsalis* are 16.7/8.8 and 12.7/10.9 mm. The mean length/width of m1–2 for *T. taoensis* are 19.8/10.4 and 14.1/11.5 mm (Simmons 1987); the same dimensions are 16/8 and 13/9.9 mm for *T. lamberti* (Simmons 1987) and 13.6/7.3 and 14.1/11.6 mm for *Sphenopsalis.* The length ratio of M2 to M1 is 0.63 for *T. taoensis* and 0.76 for *Sphenopsalis,* indicating that M1 of *T. taoensis* is proportionally longer than that of *Sphenopsalis.* The length ratio of m2 to m1 is 0.71 for *T. taoensis*, 0.81 for *T. lamberti,* and 1.04 for *Sphenopsalis*; these ratios indicate that m1 of *Taeniolabis* is proportionally much longer than that of *Sphenopsalis*, or M1 and m1 lengths are subequal in *Sphenopsalis*. Moreover, the width ratio of m2 to m1 is 1.11 for *T. taoensis,* 1.24 for *T. lamberti* and 1.59 for *Sphenopsalis.* This indicates that m1 of *Sphenopsalis* is much narrower in relation to m2 than that of *Taeniolabis.* Such a relatively narrow and short m1 of *Sphenopsalis*, in association with the width differences on the lingual and buccal tooth cusp rows on M2/m2, reflects a distinctive occlusal pattern that differs lambdopsalids from taeniolabidids. In *Taeniolabis* and *Catopsalis* the occlusal pattern is characterized by their inflated quadrangular molar cusps that can only make end-to-end contact at the occlusal surface. The grinding motion of lower molars is therefore not restricted by the furrows of the upper molars so that some transverse motion during mastication was possible in *Taeniolabis* (Fig. 15). These large bodied species with different masticatory patterns in Asian and North American taeniolabidoids lend support to the hypothesis (Wilson et al. 2012) that an adaptive shift towards increased herbivory and body size across the Cretaceous–Paleogene (K–Pg) transition.

Conclusions

We have described new dental, cranial, and postcranial specimens of *Sphenopsalis nobilis*, which were collected from the Upper Paleocene Nomogen Formation at a locality near the escarpment of Erden (Urtyn) Obo in Erlian Basin, Inner Mongolia, China. These specimens cast new light on the morphology of the otherwise poorly represented species known since 1928. With the new morphological data and comparisons with other taeniolabidoids, particularly *Lambdopsalis*, *Prionessus*, and *Taeniolabis*, we are able to further confirm *Lambdopsalis* as a valid genus and re-establish the family Lambdopsalidae Chow and Qi, 1978. We provide an emended diagnosis for the superfamily Taeniolabidoidea, the family Lambdopsalidae, and the species *Sphenopsalis nobilis*, respectively. Using a data set consisting of 43 taxa and 102 characters, we conducted phylogenetic analyses that for the first incorporate five primary genera of Taeniolabidoidea, including Asian *Sphenopsalis*, *Lambdopsalis*, *Prionessus*, and North American *Taeniolabis* and *Catopsalis*. Our analyses identified Taeniolabidoidea as a monophyletic taxon consisting of the Asian *Lambdopsalis–Sphenopsalis* clade and the North American *Taeniolabis–Catopsalis* clade, and the Asian *Prionessus* has a relatively unstable placement within taeniolabidoids. Lambdopsalids and taeniolabidids appear to have adapted to distinct diets, as reflected by their tooth morphologies; the former are characterized by teeth with sharply crested cusps that are good for shearing, whereas the latter have heavier and more quadrate cusps suitable for crushing and grinding in mastication. As the largest body-sized representatives of known North American and Eurasian multituberculates, respectively, taeniolabidids and lambdopsalids show adaptive shifts, although in different types, towards increased herbivory and body size after the K–Pg transition.

Acknowledgements

We dedicate the work to the memory of the late Yaoming Hu, who collected some of the specimens reported in the study. We thank Bin Bai, Qian Li, Xun Jin, Ping Li, Hai Xing, Wei Zhou, Chengkai, Sun, Yan Li, Qiang Cao, Qiang Li, Wei Chen, Ping Wang, Baohua Sun, Shijie Li, Qi Li, Yongxing Wang, and Yongfu Wang (all IVPP), K. Christopher Beard (Department of Ecology and Evolutionary Biology, The University of Kansas, Lawrence, USA) and Daniel L. Gebo (Department of Anthropology, Northern Illinois University, DeKalb, USA) for assistance in the field; Wei Zhou, Shijie Li, and Qi Li (all IVPP) for preparation of specimens; Wending Zhang and Shukang Zhang (both IVPP) for assistance in SEM imaging of the specimens. We thank Jørn Harald Hurum (Natural History Museum, the University of Oslo, Norway), Alexander O. Averianov (Zoological Institute, Russian Academy of Sciences, Saint Petersburg, Russia), John P. Hunter (Department of Evolution, Ecology, and Organismal Biology, The Ohio State University, Columbus, USA), and two anonymous reviewers for critical and helpful reviews. We are especially grateful to one of the two anonymous reviewers, whose thorough comments significantly improved the writing and science of the paper. Mark D. Uhen (George Mason University, Fairfax, Virginia, USA) provided helpful editorial comments. The work was supported by the Major Basic Research Projects of MST of China (Nos. 2012CB821900), the National Natural Science Foundation of China (Nos. 4140200), the Chinese Academy of Sciences (No. KZCX2-EW-106), the Special Fund for Fossil Excavation and Preparation of Chinese Academy of

Sciences. JM's research is also supported by the American Museum of Natural History.

References

Bi, S.-D., Wang, Y.-Q., Guan, J., Sheng, X., and Meng, J. 2014. Three new Jurassic euharamiyidans reinforce early divergence of mammals. *Nature* 514: 579–584.

BGMRNMAR (Bureau of Geology and Mineral Resources of Nei Mongol Autonomous Region). 1991. Regional Geology of Nei Mongol (Inner Mongolia) Autonomous Region [in Chinese, with English abstract]. *In*: People's Republic of China Ministry of Geology and Mineral Resources (ed.), *Geological Memoirs*, *Series I 25*, 1–725. Geological Publishing House, Beijing.

Bowen, G.J., Koch, P.L., Meng, J., Ye, J., and Ting, S.-Y. 2005. Age and correlation of fossiliferous late Paleocene–early Eocene strata of the Erlian Basin, Inner Mongolia, China. *American Museum Novitates* 3474: 1–26.

Butler, P.M. 2000. Review of the early allotherian mammals. *Acta Palaeontologica Polonica* 45: 317–342.

Butler, P.M. and Hooker, J.J. 2005. New teeth of allotherian mammals from the English Bathonian, including the earliest multituberculates. *Acta Palaeontologica Polonica* 50: 185–207.

Carlson, S.J. and Krause, D.W. 1985. Enamel ultrastructure of multituberculate mammals: an investigation of variability. *Contributions from the Museum of Paleontology,The Univeristy of Michigan* 27: 1–50.

Chester, S.G.B and Sargis, E.J. 2010. Mammalian distal humeri from the Late Cretaceous of Uzbekistan. *Acta Palaeontologica Polonica* 55: 199–211.

Chow, M.-C. and Qi, T. 1978. Paleocene mammalian fossils from Nomogen Formation of Inner Mongolia [in Chinese, with English abstract]. *Vertebrata PalAsiatica* 16: 77–85.

Chow, M.-C. and Rozhdestvensky, A.K. 1960. Exploration in Inner Mongolia—a preliminary account of the 1959 field work of the Sino-Soviet Paleontological Expedition (SSPE). *Vertebrata PalAsiatica* 4: 1–10.

Chow, M.-C., Qi, T., and Li, R. 1976. Paleocene stratigraphy and faunal characters of mammalian fossils of Nomogen Commune, Si-zi-wang Qi, Nei Mongol [in Chinese, with English abstract]. *Vertebrata PalAsiatica* 14: 228–233.

Cifelli, R.L., Gordon, C.L., Lipka, T.R., and Scott, C.S. 2013. New multituberculate mammal from the Early Cretaceous of eastern North America. *Canadian Journal of Earth Sciences* 50: 315–323.

Clemens, W.A. and Kielan-Jaworowska, Z. 1979. Multituberculata. *In*: J.A. Lillegraven, Z. Kielan-Jaworowska, and W.A. Clemens (eds.), *Mesozoic Mammals: The First Two-Thirds of Mammalian History*, 99–149. University of California Press, Berkeley.

Cope, E.D. 1882. Mammalia in the Laramie Formation. *American Naturalist* 16: 830–831.

Cope, E.D. 1884. The Tertiary Marsupialia. *American Naturalist* 18: 686–697.

Dashzeveg, D. 1988. Holarctic correlation of non-marine Palaeocene–Eocene boundary strata using mammals. *Journal of the Geological Society* 145: 473–478.

Fox, R.C. 1989. The Wounded Knee Local Fauna and mammalian evolution near the Cretaceous–Tertiary boundary, Saskatchewan, Canada. *Palaeontographica Abteilung A* 208: 11–59.

Fox, R.C. 1997. Late Cretaceous and Paleocene mammals, Cypress Hills Region, Saskatchewan, and mammalian evolution across the Cretaceous–Tertiary boundary. *In*: L. McKenzie-McAnally (ed.), *Upper Cretaceous and Tertiary Stratigraphy and Paleontology of Southern Saskatchewan. Canadian Paleontology Conference, Field Trip Guidebook 6*, 70–85. Geological Association of Canada (Paleontology Division), St. John's.

Fox, R.C. 1999. The monophyly of the Taeniolabidoidea (Mammalia: Multituberculata). *In*: H.A. Leanza (ed.), *Abstracts*, *VII International Symposium on Mesozoic Terrestrial Ecosystems*, 26. Asociación Paleontológica Argentina, Buenos Aires.

Fox, R.C. 2005. Microcosmodontid multituberculates (Allotheria, Mammalia) from the Paleocene and Late Cretaceous of western Canada. *Palaeontographica Canadiana* 23: 1–109.

Fox, R.C. and Meng, J. 1997. An X-radiographic and SEM study of the osseous inner ear of multituberculates and monotremes (Mammalia): implications for mammalian phylogeny and evolution of hearing. *Zoological Journal of the Linnean Society* 121: 249–291.

Granger, W. 1928. *Records of Fossils, Mongolia 1928. Third Central Asiatic Expeditions (Field Notes)*. 79 pp. American Museum of National History, New York.

Granger, W. and Simpson, G.G. 1929. A revision of the Tertiary Multituberculata. *Bulletin of the American Museum of Natural History* 56: 601–676.

Hahn, G. 1969. Beiträge zur Fauna der Grube Guimarota Nr. 3. Die Multituberculata. *Palaeontographica Abteilung A* 133: 1–100.

Hahn, G. and Hahn, R. 1998a. Neue Beobachtungen an Plagiaulacoidea (Multituberculata) des Ober-Juras. 2. Zum Bau des Unterkiefers und des gebisses bei Meketibolodon und bei Guimarotodon. *Berliner geowissenschaftliche Abhandlungen E* 28: 9–37.

Hahn, G. and Hahn, R. 1998b. Neue Beobachtungen an Plagiaulacoidea (Multituberculata) des Ober-Juras. 3. Der Bau der Molaren bei den Paulchoffatiidae. *Berliner geowissenschaftliche Abhandlungen E* 28: 39–84.

Hurum, J.H. 1998. The Inner Ear of Two Late Cretaceous Multituberculate Mammals, and Its Implications for Multituberculate Hearing. *Journal of Mammalian Evolution* 5: 65–93.

Jenkins, P.A. Jr. and Weijs, W.A. 1979. The functional anatomy of the shoulder in the Virginia opossum (*Didelphis virginiana*). *Journal of Zoology* 188: 379–410.

Jiang, H.-X. 1983. Division of the Paleogene in the Erlian basin of Nei Mongol [in Chinese]. *Geology of Nei Mongol* 2: 18–36.

Kielan-Jaworowska, Z. 1969. New Upper Cretaceous multituberculate genera from Bayn Dzak, Gobi Desert. *Palaeontologia Polonica* 21: 35–49.

Kielan-Jaworowska, Z. 1971. Skull structure and affinities of the Multituberculata. *Palaeontologia Polonica* 25: 5–41.

Kielan-Jaworowska, Z. 1974. Multituberculate succession in the Late Cretaceous of the Gobi Desert (Mongolia). *Palaeontologica Polonica* 30: 23–44.

Kielan-Jaworowska, Z. 1980. Absence of ptilodontoidean multituberculates from Asia and its palaeogeographic implications. *Lethaia* 13: 169–173.

Kielan-Jaworowska, Z. 1989. Postcranial skeleton of a Cretaceous multituberculate mammal. *Acta Palaeontologica Polonica* 34: 75–85.

Kielan-Jaworowska, Z. and Dashzeveg, D. 1978. New Late Cretaceous mammal locality in Mongolia and a description of a new multituberculate. *Acta Palaeontologica Polonica* 23: 115–130.

Kielan-Jaworowska, Z. and Gambaryan, P.P. 1994. Postcranial anatomy and habits of Asian multituberculate mammals. *Fossils and Strata* 27: 17–31.

Kielan-Jaworowska, Z. and Hurum, J.H. 2001. Phylogeny and systematics of multituberculate mammals. *Palaeontology* 44: 389–429.

Kielan-Jaworowska, Z. and Qi, T. 1990. Fossorial adaptations of a taeniolabidoid multituberculate mammal from the Eocene of China. *Vertebrata PalAsiatica* 28: 81–94.

Kielan-Jaworowska, Z. and Sloan, R.E. 1979. *Catopsalis* (Multituberculata) from Asia and North America and the problem of taeniolabidid dispersal in the Late Cretaceous. *Acta Palaeontologica Polonica* 24: 187–197.

Kielan-Jaworowska, Z., Cifelli, R.L., and Luo, Z.X. 2004. *Mammals from the Age of Dinosaurs: Origins, Evolutions, and Structure*. 630 pp. Columbia University Press, New York.

Krause, D.W. and Hahn, G. 1990. Systematic position of the Paulchoffatiinae (Multituberculata, Mammalia). *Journal of Paleontology* 64: 1051–1054.

Krause, D.W. and Jenkins, F.A. Jr. 1983 The postcranial skeleton of North American multituberculates (Mammalia). *Bulletin of the Museum of Comparative Zoology, Harvard University* 150: 199–246.

Lucas, S.G., Williamson, T.E., and Middleton, M.D. 1997. *Catopsalis* (Mammalia: Multituberculata) from the Paleocene of New Mexico and Utah: taxonomy and biochronological significance. *Journal of Paleontology* 71: 484–493.

Luo, Z.-X. and Ketten, D.R. 1991. CT scanning and computerized recon-

structions of the inner ear of multituberculate mammals. *Journal of Vertebrate Paleontology* 11: 220–228.
Luo, Z.-X., Kielan-Jaworowska, Z., and Cifelli, R.L. 2002. In quest for a phylogeny of Mesozoic mammals. *Acta Palaeontologica Polonica* 47: 1–78.
Luo, Z.-X., Yuan, C.-X., Meng, Q.-J., and Ji, Q. 2011. A Jurassic eutherian mammal and divergence of marsupials and placentals. *Nature* 476: 442–445.
Matthew, W.D. and Granger, W. 1925. Fauna and correlation of the Gashato Formation of Mongolia. *American Museum Novitates* 189: 1–12.
Matthew, W.D., Granger, W., and Simpson, G.G. 1928. Paleocene multituberculates from Mongolia. *American Museum Novitates* 331: 1–4.
McKenna, M.C. 1961. On the shoulder girdle of the mammalian subclass Allotheria. *American Museum Novitates* 2066: 1–27.
McKenna, M.C. 1975. Toward a phylogenetic classification of the Mammalia. *In*: W.P. Luckett, and F.S. Szalay (eds.), *Phylogeny of the Primates*, 21–46. Cambridge University Press, Cambridge.
McKenna, M.C. and Bell, S.K. 1997. *Classification of Mammals: Above the Species Level*, 1–631. Columbia University Press, New York.
Meng, J. 1992. The stapes of *Lambdopsalis bulla* (Multituberculata) and transformational analyses on some stapedial features in Mammaliaformes. *Journal of Vertebrate Paleontology* 12: 459–471.
Meng, J. 2014. Mesozoic mammals of China: implications for phylogeny and early evolution of mammals. *National Science Review* 1: 521–542.
Meng, J. and McKenna, M.C. 1998. Faunal turnovers of Palaeogene mammals from the Mongolian Plateau. *Nature* 394: 364–367.
Meng, J. and Wyss, A.R. 1995. Monotreme affinities and low-frequency hearing suggested by multituberculate ear. *Nature* 377: 141–144.
Meng, J., Bi, S.-D., Zheng, X.-T., and Wang, X.-L. 2014. Dental and mandibular morphologies of *Arboroharamiya* (Haramiyida, Mammalia): comparisons with other haramiyidans and *Megaconus* and implications for mammalian evolution. *PLoS ONE* 9 (12): e113847.
Meng, J., Hu, Y.-M., and Li, C.-K. 2003. The osteology of *Rhombomylus* (Mammalia, Glires) and its implication for Glires systematics and evolution. *Bulletin of the American Museum of Natural History* 275: 1–247.
Meng, J., Wang, Y.-Q., Ni, X.-J., Beard, K.C., Sun, C.-K., Li, Q., Jin, X., and Bai, B. 2007. New stratigraphic data from the Erlian Basin: Implications for the division, correlation, and definition of Paleogene lithological units in Nei Mongol (Inner Mongolia). *American Museum Novitates* 3570: 1–31.
Meng, J., Wyss, A.R., Dawson M., and Zhai R.-J., 1994. Primitive fossil rodent from Inner Mongolia and its implications for mammalian phylogeny. *Nature* 370: 134–136.
Meng, J., Zhai, R.-J., and Wyss, A.R. 1998. The late Paleocene Bayan Ulan fauna of Inner Mongolia, China. *In*: K.C. Beard and M.R. Dawson (eds.), Dawn of the Age of Mammals in Asia. *Bulletin of Carnegie Museum of Natural History* 34: 148–185.
Miao, D.-S. 1986. Dental anatomy and ontogeny of *Lambdopsalis bulla* (Mammalia, Multituberculata). *Contributions to Geology, University of Wyoming* 24: 65–76.
Miao, D.-S. 1988. Skull morphology of *Lambdopsalis bulla* (Mammalia, Multituberculata) and its implications to mammalian evolution. *Contributions to Geology, University of Wyoming, Special Paper* 4: 1–104.
Miao, D.-S. and Lillegraven, J. 1986. Discovery of three ear ossicles in a multituberculate mammal. *National Geographic Research* 2: 500–507.
Middleton, M.D. 1982. A new species and additional material of *Catopsalis* (Mammalia, Multituberculata) from theWestern Interior of North America. *Journal of Paleontology* 56: 1197–1206.
Missiaen, P. and Smith, T. 2008. The Gashatan (late Paleocene) mammal fauna from Subeng, Inner Mongolia, China. *Acta Palaeontologica Polonica* 53: 357–378.
Osborn, H.F. 1929. *Embolotherium*, gen. nov., of the Ulan Gochu, Mongolia. *American Museum of Natural History* 335: 1–20.
Qi, T. 1987. The middle Eocene Arshanto fauna (Mammalia) of Inner Mongolia. *Annals of Carnegie Museum* 56: 1–73.
Qi, T. 1990. A Paleogene section at Erden Obo, Nei Mongol and on the discovery of *Pastoralodon lacustris* (Pantodonta, Mammalia) in that area [in Chinese with English summary]. *Verterata PalAsiatica* 28: 25–33.
Radinsky, L.B. 1964. Notes on Eocene and Oligocene fossil localities in Inner Mongolia. *American Museum Novitates* 2180: 1–11.
Rougier, G.W., Novacek, M.J., and Dashzeveg, D. 1997. A new multituberculate from the late Cretaceous locality Ukhaa Tolgod, Mongolia: considerations on multituberculate interrelationships. *American Museum Novitates* 3191: 1–26.
Russell, D.E. and Zhai, R.-J. 1987. The Paleogene of Asia: mammals and stratigraphy. *Mémoires du Muséum National d'Histoire Naturelle, Série C: Sciences de la Terre* 52: 1–448.
Sereno, P.C. and McKenna, M.C. 1995. Cretaceous multituberculate skeleton and the early evolution of the mammalian shoulder girdle. *Nature* 377: 144–147.
Simmons, N.B. 1987. A revision of *Taeniolabis* (Mammalia: Multituberculata), with a new species from the Puercan of eastern Montana. *Journal of Paleontology* 61: 794–808.
Simmons, N.B. 1993. Phylogeny of Multituberculata. *In*: F.S. Szalay, M.J. Novacek, and M.C. McKenna (eds.), *Mammal Phylogeny: Mesozoic Differentiation, Multituberculates, Monotremes, Early Therians, and Marsupials*, 146–164. Springer Verlag Press, New York.
Simmons, N.B. and Miao, D.-S. 1986. Paraphyly in *Catopsalis* (Mammalia: Multituberculata) and its biogeographic implications. *Contributions to Geology, University of Wyoming* 24 (Special Paper 3): 87–94.
Simpson, G.G. 1928. Further notes on Mongolian Cretaceous mammals. *American Museum of Natural History* 329: 1–14.
Simpson, G.G. 1929. Amercian Mesozoic Mammalia. *Memoirs of the Peabody Museum of Yale University* 3: 1–235.
Simpson, G.G. 1937. Skull structure of the Multituberculata. *Bulletin of the American Museum of Natural History* 73: 727–763.
Sloan, R.E. and Van Valen, L. 1965. Cretaceous mammals from Montana. *Science* 148: 220–227.
Swofford D.L. 2002. *PAUP: Phylogenetic Analysis Using Parsimony, Version 4.0b10*. Sinauer Associates, Inc., Sunderland.
Van Valen, L. 1976. Note on the origin of multituberculates (Mammalia). *Journal of Paleontology* 50: 198–199.
Wang, Y.-Q., Meng, J., and Jin, X. 2012. Comments on Paleogene localities and stratigraphy in the Erlian basin, Nei Mongol, China [in Chinese, with English abstract]. *Vertebrata PalAsiatica* 50: 181–203.
Wang, Y.-Q., Meng, J., Beard, C.K., Li, Q., Ni, X., Gebo, D.L., Bai, B., Jin, X., and Li, P. 2010. Early Paleogene stratigraphic sequences, mammalian evolution and its response to environmental changes in Erlian Basin, Inner Mongolia, China. *Science China Earth Sciences* 53: 1918–1926.
Weil, A. 1998. A new species of *Microcosmodon* (Mammalia: Multituberculata) from the Paleocene Tullock Formation of Montana, and an argument for the Microcosmodontinae. *Museum of Paleontology, University of California* 18 (2–3): 1–39.
Wible, J.R. and Rougier, G.W. 2000. Cranial anatomy of *Kryptobaatar dashzevegi* (Mammalia, Multituberculata), and its bearing on the evolution of mammalian characters. *Bulletin of the American Museum of Natural History* 247: 1–120.
Wilson, G.P. 2012. Mammals across the K/Pg boundary in northeastern Montana, U.S.A.: dental morphology and body-size patterns reveal extinction selectivity and immigrant-fueled ecospace filling. *Paleobiology* 39: 429–469.
Wilson, G.P., Evans, A.R., Corfe, I.J., Smits, P.D., Fortelius, M., and Jernvall, J. 2012. Adaptive radiation of multituberculate mammals before the extinction of dinosaurs. *Nature* 483: 457–460.
Wilson, R.W. 1987. Late Cretaceous (Fox Hills) multituberculates from the Red Owl local fauna of western North Dakota. *Dakoterra* 3: 118–132.
Yuan, C.-X., Ji, Q., Meng, Q.-J., Tabrum, A.R., and Luo, Z.-X. 2013. Earliest evolution of multituberculate mammals revealed by a new Jurassic fossil. *Science* 341: 779–783.
Zheng, X.-T., Bi, S.-D., Wang, X.-L., and Meng, J. 2013. A new arboreal haramiyid shows the diversity of crown mammals in the Jurassic period. *Nature* 500: 199–202.